

A normative account of the trade-off between cognitive stability and flexibility

Tromp, J.<sup>1,2</sup>, Nieuwenhuis, S.<sup>1</sup>, Cohen, J. D.<sup>3</sup>, & Jongkees, B. J.<sup>1\*</sup>

<sup>1</sup> Institute of Psychology, Leiden University, Leiden, The Netherlands

<sup>2</sup> Donders Institute, Radboud UMC, Nijmegen, The Netherlands

<sup>3</sup> Princeton Neuroscience Institute, Princeton University, Princeton, U.S.A.

\* Corresponding author: b.j.jongkees@fsw.leidenuniv.nl

Word count abstract: 206

Word count main text (excl. reference list): 18234

## Abstract

Optimal decision making often requires a compromise between opposing functional demands. This is illustrated by the extensive literature that focuses on the optimal trade-off between response speed versus accuracy. However, a formally rigorous, normative account of the trade-off between cognitive stability versus flexibility is still lacking. In this article, we provide such an account and consider how these two trade-offs can be jointly optimized. We present a mechanistic process model of task switching, in which attractor dynamics of control induce a trade-off between stable processing and flexible reconfiguration. A behavioral experiment shows that human participants broadly conform to normative model predictions and that changes in their control dynamics are accompanied by changes in neurophysiological markers of cognitive flexibility. Crucially, we find that such optimization of control is not always reflected in traditional behavioral measures of stability and flexibility. We suggest that relying exclusively on these behavioral measures can explain recent proposals that stability and flexibility can vary independently. More broadly, we argue that hypotheses on the nature of control should be developed and tested using formally rigorous, mechanistically precise models that can make quantitative predictions, capture individual differences, and account for the complex interactions that can occur among multiple, often subtle factors that influence decision-making processes.

Key words: stability-flexibility, speed-accuracy, cognitive control, optimal performance, non-linear dynamical system

## 1. Introduction

People rely on cognitive control to adapt their information processing and decision making in a context-appropriate manner. For example, situations can vary in their optimal trade-offs between stability versus flexibility of attention (Cools, 2019; Goschke, 2003; Musslick & Cohen, 2021) and speed versus accuracy of responding (Balci et al., 2011; Bogacz et al., 2006). Adaptation of these trade-offs is crucial to healthy behavior and often impaired in psychopathology (Millan et al., 2012), which has spurred great interest in the mechanisms of adaptive control.

Context-sensitive control is often studied using task-switching paradigms, in which participants alternate between performing different tasks (Dreisbach & Haider, 2006; Egner, 2017; Monsell, 2003). Successful performance requires managing the trade-off between stable focus on the current task to minimize distraction and cross-task interference, versus flexible disengagement from and switching between tasks. Participants exhibit faster task switching in contexts requiring more frequent switches, albeit at the expense of increased cross-task interference (Dreisbach & Fröber, 2019; Qiao et al., 2023). This suggests that participants are subject to a stability-flexibility trade-off that they adapt to contextual demands.

To understand the mechanisms underlying such adaptation, computational modeling approaches have framed adaptive control as a problem of performance optimization (Jongkees et al., 2023; Musslick et al., 2019, 2018). These models simulate information processing in cognitive tasks as a process of noisy evidence accumulation over time, by which a response is selected when the evidence favoring one alternative reaches a specified threshold. Control signals serve to bias evidence accumulation in line with task goals, such that strong intensity of control signals augment and narrow processing to task-relevant inputs, but at the expense of slower reconfiguration of the control signals when the task switches. Conversely, weaker intensity of control allows faster reconfiguration, but at the cost of a greater influence of task-

irrelevant inputs. These dynamics of control have been formalized as attractor basins in a potential energy landscape, with deep attractors conferring greater stability but also increasing the distance between attractors (Durstewitz & Seamans, 2008; Musslick & Cohen, 2021; Ueltzhöffer et al., 2015). Model simulations indicate that when task-switches are frequent, optimal performance (in terms of maximizing response accuracy) can be achieved through weaker intensity of control (Musslick et al., 2018) – that is, a more shallow attractor landscape. This produces behavior similar to that observed in humans: improved switching but greater cross-task interference.

The work outlined above provided a useful starting point for considering how optimal intensity of control may be sensitive to the demand for flexibility. However, by focusing exclusively on maximizing response accuracy, it did not address another key aspect of optimal control: the speed-accuracy trade-off. There is considerable evidence that this trade-off, like stability versus flexibility, is subject to strategic control; people seek to optimize this trade-off in order to maximize average reward rate (RR), calculated as the proportion of accurate trials divided by the average response time (Bogacz et al., 2006; Gold & Shadlen, 2002). Based on evidence accumulation models of decision making (e.g. Ratcliff, 1978), it can be shown that RR is suboptimal for very fast, inaccurate responses as well as very slow, accurate ones, while there is an optimal speed-accuracy trade-off (usually expressed in terms of the threshold of the accumulation process) that maximizes the average RR (Bogacz et al., 2006).

The speed-accuracy trade-off must always be considered when using behavioral measures to test hypotheses about the cognitive processes responsible for performance of a given task, and using task-switching behavior to study the stability-flexibility trade-off is no exception. For example, previous work has shown that faster switching between tasks may simply reflect a favoring of speed over accuracy, through the use of a lower threshold during evidence accumulation, rather than favoring of flexibility over stability (Jongkees et al., 2023). Such

threshold reduction effectively reduces the response time (RT) difference between repeat vs switch trials, which is often the primary outcome measure in task-switching studies. Because accuracy rates can still be high and frequently violate assumptions of common statistical tests, a decrease in accuracy is not guaranteed to be detected. In other words, without careful joint analysis of response speed and accuracy, favoring speed over accuracy can be mistakenly interpreted as favoring of flexibility over stability.

Two additional factors are also important when considering the interaction between the speed-accuracy and stability-flexibility trade-offs. The first is that, whereas threshold is commonly assumed to be static during evidence accumulation, there is mounting evidence that it may often be adjusted within the course of a trial (Ditterich, 2006; Thura et al., 2012). Specifically, it has been proposed that as time passes and a response has not been made, urgency builds up and progressively “collapses” the decision threshold. This avoids long RTs, which is especially relevant when there is a strict response deadline. However, the optimality of such a collapsing threshold remains debated. Some have suggested it maximizes RR (Drugowitsch et al., 2012; Frazier & Yu, 2007), while others have indicated this is true only for difficult tasks and to a relatively minor benefit, with static thresholds remaining an effective default (Boehm et al., 2020). Thus, to comprehensively characterize how control is optimized for the demand of flexibility, it is relevant to consider potential effects of within-trial urgency and corresponding adjustment of decision threshold, and how this might differentially impact performance when repeating versus switching tasks.

The second factor to consider is that people often fail to achieve an optimal RR due, in part, to an emphasis on accuracy as well as RR. This can be formalized as:

$$RR_q = \frac{Accuracy - q * (1 - Accuracy)}{RT} \quad (1)$$

where  $q$  is a cost parameter that penalizes the RR for errors above and beyond the opportunity cost of time (when  $q = 0$  this equation reduces to the standard RR, reflecting no additional sensitivity to errors). Formal analyses have shown that the RR-maximizing threshold is higher for higher values of  $q$  (Bogacz et al., 2006). Empirical results indicate that many participants exhibit such additional sensitivity to errors but that this decreases with practice, which is associated with progressively higher RRs (Balci et al., 2011; Bogacz et al., 2010). Given that task switching is associated with relatively slow and error-prone performance, it is possible that the optimal stability-flexibility trade-off is influenced by people's sensitivity to errors that manifests as correspondingly higher thresholds.

### **Aim and approach**

In this paper we consider all of the factors outlined above, with the goal of providing a normative account of how control is deployed in task-switching settings in order to maximize RR, by simultaneously optimizing the stability-flexibility and speed-accuracy trade-offs, while taking account of the potential effects of time-varying urgency and heightened sensitivity to errors. In doing so, we also address recent suggestions that stability and flexibility do not necessarily trade off against each other (Egner, 2023; Mayr & Grätz, 2024). As we discuss in more detail later, a key difference between these suggestions and our approach is that the former relies heavily on behavioral measures of stability and flexibility, whereas ours focuses on the underlying mechanisms that drive behavior. The argument that stability and flexibility do not necessarily trade off against each other is based on the observation that behavioral measures traditionally used to index stability (incongruence costs) and flexibility (switch costs) can, under some conditions, both increase or decrease together rather than trading off against each other. In contrast, here we formulate stability and flexibility not in terms of behavioral measures, which can also reflect factors unrelated to stability-flexibility (e.g., the speed-

accuracy trade-off), but rather in terms of functional attributes of underlying processing mechanisms.

Specifically, we define stability as the strength with which representations responsible for performance of a particular task are expressed in the system, such that stronger expression is associated with better performance. In principle, this formulation allows multiple such representations to be expressed strongly at the same time, and thus two or more tasks to be performed well at the same time, so long as they are compatible – that is, so long as they do not interfere directly with one another, or produce downstream interference that degrades performance of one or the other task. Indeed, a rich body of literature on multi-tasking has examined under which circumstances it is possible for different tasks to be performed simultaneously or in rapid succession without degrading performance (Meyer & Kieras, 1997; Musslick & Cohen, 2021; Pashler, 1994; Shiffrin & Schneider, 1977)

However, *incompatible* tasks – that involve bivalent stimuli and overlapping response sets – are a key design feature of the behavioral paradigms used to study task switching (Allport et al., 1994; Kiesel et al., 2010; Meiran, 1996; Monsell, 2003) and address the relationship between stability and flexibility (Egner, 2023; Mayr & Grätz, 2024). By definition, such incompatibility means that both task representations cannot be expressed maximally without producing interference, and thus performance cannot be optimal for both tasks at the same time. That is, by design, focusing on conditions in which tasks interfere with one another introduces a tension between stability (optimal performance of each task) and flexibility – the ability to transition between task representations in order to optimize performance for one or the other. As we show in this paper, a formalization of stability and flexibility in these terms affords both a mechanistically explicit and normative account of cognitive function in terms of the stability-flexibility trade-off, and predicts several of the behavioral observations that have been used to argue against the trade-off at the mechanistic level. Our approach therefore suggests a

reconciliation between concerns about the stability-flexibility trade-off viewed strictly through the lens of behavioral measures, and its relevance at the level of underlying mechanisms.

To capture the complex and possibly non-linear interactions among all the factors discussed above, we rely on a mechanistic process model of task switching developed by Jongkees et al. (2023). We use this model first to address how task-switching performance varies as a function of the stability-flexibility and speed-accuracy trade-offs. We then use it to derive normative predictions concerning optimal, RR-maximizing control parameters as a function of the contextual demand for flexibility (i.e., the frequency of task-switches). Finally, we test these predictions of the model in a behavioral experiment. To provide further insight into how adaptive control is realized, we also examine biological correlates of the cognitive and computational mechanisms described above. At a neurophysiological level, it has been proposed that an important function of catecholamine systems is to optimize processing by modulating neural gain in order to regulate control dilemma's (Aston-Jones & Cohen, 2005; Eldar et al., 2013; Ferguson & Cardin, 2020). While recent research has linked catecholaminergic activity more directly to the stability-flexibility trade-off (Cools, 2019), the underlying mechanisms (e.g., global gain modulation) are often indirectly inferred rather than explicitly modeled.

Here we focus on one particular catecholaminergic system — the locus coeruleus (LC) — based on a growing body of evidence suggesting a role for this system in cognitive control (Aston-Jones & Cohen, 2005; Bouret & Sara, 2005; McBurney-Lin et al., 2022). The LC exerts a global influence across extensive regions of the brain by modulating neural gain through its noradrenergic projections. Furthermore, it has been found that these effects can be non-invasively indexed using pupil diameter (Breton-Provencher & Sur, 2019; de Gee et al., 2017; Gilzenrat et al., 2010; Lloyd et al., 2023; Reimer et al., 2016). For example, increased baseline pupil size has been linked to behavioral measures of task disengagement and exploration, two

behavioral signatures of cognitive flexibility (Devauges & Sara, 1990; Gilzenrat et al., 2010; Hayes & Petrov, 2016; Jepma & Nieuwenhuis, 2011; Lapiz et al., 2007; Pajkossy et al., 2018; Seu et al., 2009).

More direct neurophysiological measurements, using scalp electrical recordings (electroencephalography, or EEG), have suggested that regulation of the stability-flexibility trade-off may be reflected in posterior alpha power, an EEG index of cognitive effort and task engagement (Klimesch et al., 2007; Macdonald et al., 2011). Alpha power is typically suppressed during periods of high control intensity, for example after response conflict (Compton et al., 2011) or during preparation for an upcoming task switch (Gladwin & de Jong, 2005; Kaiser et al., 2023). Interestingly, there is preliminary evidence for *reduced* suppression of posterior baseline alpha power in contexts where task switches are frequent (Liu & Yeung, 2020); but see (Siqi-Liu et al., 2022). This raises the possibility that reduced suppression of baseline alpha power reflects adjustments of control intensity, but previous work has not explicitly investigated this hypothesis.

## Overview

In Section 2 we describe a mechanistic process model, in the form of a non-linear dynamical system (Jongkees et al., 2023), that we use to quantify how task-switching performance changes as a function of the stability-flexibility and speed-accuracy trade-offs. We model changes in these two trade-offs through the use of three control parameters that we assume can be strategically adjusted to contextual task demands: the stability-flexibility trade-off is governed by the gain of control signals that bias the processing of stimuli ('control signal intensity'), while the speed-accuracy trade-off is governed both by the initial threshold during evidence accumulation ('response caution') and its collapse rate over the course of evidence accumulation ('time-varying urgency'). We show that gain and threshold often exhibit a non-

monotonic relationship to performance under varying task conditions and error sensitivities, suggesting that there is an optimal level of these control parameters (i.e., that maximizes RR) in a given context, and that can be used to make normative predictions about behavior.

In Section 3 we formally test this idea by examining if and how optimal (i.e., RR-maximizing) control parameters depend on the demand for flexibility – that is, the frequency of task-switches. Consistent with prior work (Musslick et al., 2019, 2018), we show that the optimal gain of control signals is lower when the frequency of task-switches is high. At the same time, optimal regulation of threshold (initial level and within-trial adjustments) depends on the sensitivity of errors: When task-switches are frequent, higher initial thresholds combined with more rapid collapse are optimal, but only when error sensitivity is high and only yielding a relatively small increase in RR. These findings reaffirm that optimizing control with respect to both trade-offs depends on the frequency of task-switches.

Finally, in Section 4 we report empirical results from a behavioral experiment ( $N = 35$ ) that indicate participants conform to the normative predictions of the model. Specifically, model-fitted gain is lower when task-switch frequency is high, while model-fitted initial thresholds indicate that participants optimize a combination of RR and accuracy, and neither threshold nor collapse rate is adapted to task-switch frequency. Neurophysiological results indicate that the adjustment of gain to the frequency of task-switches is accompanied by distinct changes in pupil size and EEG alpha power.

Throughout these sections and the General Discussion, we consider potential implications of these computational, behavioral, and neurophysiological findings.

## 2. Task Switching in a Dynamical System Model

The model we present is based on the non-linear dynamical system model introduced by Musslick et al. (2018), and extended by Jongkees et al. (2023), and adapted to model performance in a standard task-switching paradigm. As context, we begin by describing the task design. We then describe the model, followed by simulations of the task using the model.

### Task design

The model was designed to simulate performance of a general form of two alternative, forced-choice (2AFC) decision making in the context of a task-switching design. On each trial the model was presented with a stimulus for which one of two possible responses had to be selected, according to one of two task rules. A task cue was presented some amount of time before the stimulus, to indicate which of the two tasks should be performed. For the sake of illustration, and in line with our behavioral experiment, we focus on the often-used parity-magnitude task-switching paradigm (Figure 1), in which a single digit ranging from 1 through 9 excluding 5 must be categorized either as being odd versus even (parity task) or smaller versus larger than 5 (magnitude task). Trial to trial variation of the task cue implements task-repeat and task-switch trials, creating a need for flexible reconfiguration of control. Moreover, mapping the two tasks onto the same response options (“left” for odd and small responses, “right” for even and larger responses) implements response-congruent and response-incongruent trials, creating a need for managing potential cross-task interference.

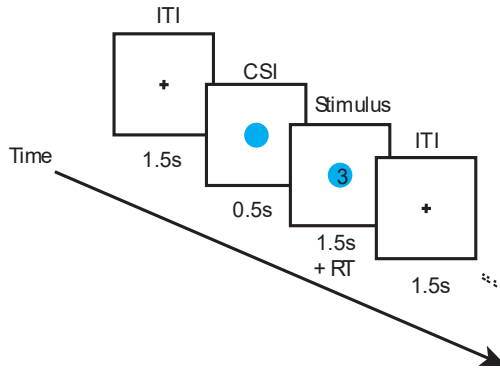


**Figure 1.** Example of a trial in the parity-magnitude task-switching paradigm. ITI = inter-trial interval, CSI = cue-stimulus interval. The timings per trial correspond to the timings in our empirical experiment.

## Model description

The model was implemented and simulations were conducted using the Python package PsyNeuLink ([psyneulink.org](https://psyneulink.org)), which provides a block modeling environment for constructing and simulating complex, interactive models, and fitting them to data using relevant objective functions.

*Model architecture.* The model (Figure 2a) was a neural network that integrated a well-established mechanism underlying decision making (Bogacz et al., 2006; Ratcliff, 1978) with a control mechanism that determined the strength with which different task representations were expressed and thereby regulated how strongly each of two sources of information about the stimulus (e.g., its parity and magnitude) determined the outcome of the decision-making process (Cohen et al., 1990; Kalanthroff et al., 2018; Musslick & Cohen, 2021). Each of these was relevant for one task and not the other. The decision mechanism accumulated noisy evidence about *both* of the two stimulus dimensions over time, weighted by the control signals, and generated a response when evidence favoring of one of the two response alternatives crossed a threshold. The height of the threshold regulated the speed-accuracy trade-off, with

lower thresholds producing faster, less accurate responses (i.e., lower response caution). Crucially, control units dynamically regulated activity in each of the two pathways that conveyed stimulus information to the decisions mechanism, with the activity of and competition between control units responsible for each dimension (and corresponding task) determining the

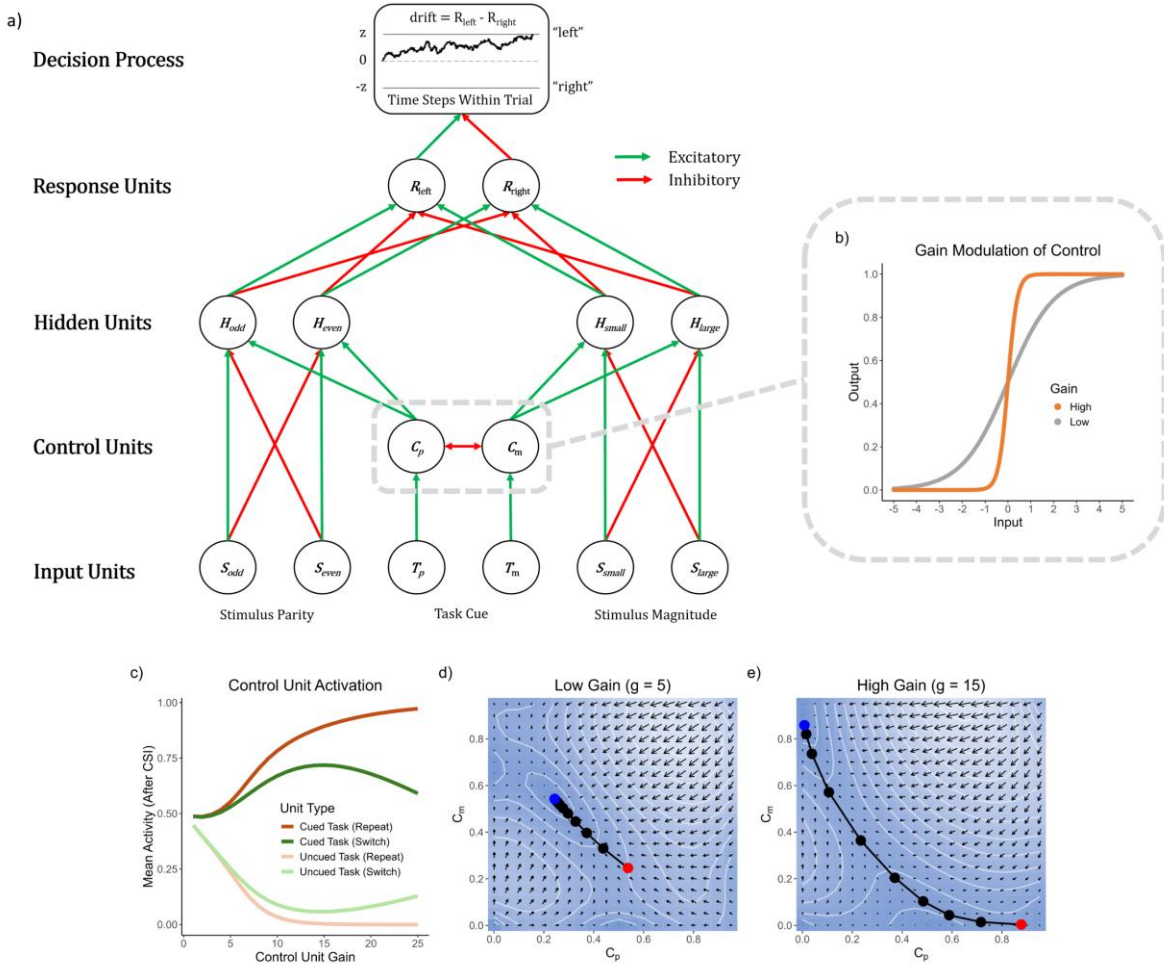


**Figure 2. Non-linear dynamical system model of task-switching.** (a) Network architecture. The activity of task-representing control units ( $C_p$  = parity,  $C_m$  = magnitude) unfolds over the course of a trial, and is determined by excitatory task cue input, mutual inhibition, decay, and gain modulation (see Equations 2 and 3). The control units increase activity of the corresponding hidden processing units ( $H_i$ ) that represent the four possible stimulus features. The hidden units provide input to two response units ( $R_i$ ) which, in turn, provide input to a decision process implemented as a drift diffusion model (DDM). On each trial, the DDM accumulates evidence based on the difference in activity of the two response units until a threshold is reached. (b) Effect of gain modulation on the nonlinear activation function of control units, relating its activity to its net input. (c) Effect of gain modulation on the average control unit activity for the cued and uncued task during evidence accumulation on switch versus repeat trials. Unit activity was averaged during 0.5s of evidence accumulation, after a CSI of 0.5s, with one cycle of processing (timestep) executed for each .01 s. (d-e) Phase portraits for activity of the control units in response to inputs from task cues  $T_i$ , under low gain (d) and high gain (e), showing trajectory from prior activation of one task (e.g., red dot for  $C_p$ ) to the cued task (e.g., blue for  $C_m$ ). Contour lines and arrows indicate the energy and shape of the attractor landscape after a task switch, black dots show the unit activations at every 10 timesteps.

dynamics of task performance, and regulating the trade-off between flexible task switching and cross-task interference: Stronger, slow-changing control signals augmented and narrowed stimulus processing to the task-relevant stimulus input (“stability”), whereas weaker, faster-changing control signals allowed broader integration of both stimulus inputs (“flexibility”) but at the potential expense of compromising task performance.

*Representations and processing.* On each trial, the cued task (parity or magnitude) was encoded by binary input units  $T$ , indexed by task  $i \in \{1,2\}$ . Similarly, input units  $S$  represented the task-relevant stimulus features along each dimension (i.e., parity and magnitude relative to 5) and encoded these as binary values (i.e., representing odd/even for parity input units and smaller/larger than 5 for magnitude input units). These units were indexed by  $i, j \in \{1,2\}$ , where again  $i$  is the task and  $j$  is the stimulus feature.

The task inputs  $T$  projected to control units  $C$ , which represented the intensity of control signals for each task, indexed by task  $i \in \{1,2\}$ . The control units were leaky competing accumulators (Usher & McClelland, 2001) and their activity was driven by their respective net inputs:

$$dnet_i = \frac{dt}{\tau} [T_i - \lambda \cdot net_i - \beta \cdot C_{i^*}], \quad i^* \neq i \quad (2)$$

where  $T$  is the unit’s corresponding task cue input, set to 1 if the task is cued and 0 otherwise;  $\lambda$  is the decay rate, reflecting passive leakage of activation over time and is fixed to 7;  $\beta$  is the inhibitory weight applied to the activity of the competing control unit  $i^*$  and is fixed to 3;  $\tau$  is the time step size, fixed to 0.01. The net input of each control unit was related to its activity state by a nonlinear (logistic) activation function:

$$C_i = \frac{1}{1 + e^{-g \cdot net_i}} \quad (3)$$

where  $g$  is a gain parameter that amplifies input and constrains the minimum and maximum levels of activity (Figure 2b). In the limit, control unit activity was constrained between 0 and 1.

Task preparation during the cue-stimulus interval (CSI) – that is, after the onset of the task cue and before the onset of the target stimulus – was modeled by allowing the control units to process their task inputs  $T$  for a fixed number of timesteps (cycles of processing) before the other model units executed. In all simulations and in our behavioral experiment, we used a CSI of 0.5 seconds (s), with a correspondence of 0.01 s in real time to 1 timestep in the model. Thus, the control units executed 50 times during the CSI of 0.5 s.

Subsequently, the stimulus was presented to the model, providing input to the features of each task (odd and even in the parity pathway; small and large in the magnitude pathway) and were indexed by task  $i \in \{1,2\}$  and stimulus feature  $j \in \{1,2\}$ . The hidden units  $H$  processed this input, along with their input from the control units, with the net input to each hidden unit $_{ij}$  given by:

$$net_{i,j} = \omega \cdot (S_{i,j} - S_{i,j^*}) + 4 \cdot C_i - 4, j^* \neq j \quad (4)$$

where  $S_{i,j}$  is the unit's corresponding stimulus input (e.g., “odd” in the parity pathway), set to 1 if the feature is present and 0 otherwise;  $S_{i,j^*}$  is the alternative stimulus input for that task (e.g., “even” in the parity pathway); weight  $\omega$  is the weight assigned to each stimulus input (fixed to 1);  $C_i$  is the activity of the control unit for the corresponding task, that was multiplied by a fixed weight of 4; and each unit was given a constant negative bias of -4. The purpose of the negative bias was to ensure that hidden units were inactive in the absence of input, and activated only weakly by stimulus input unless they also received sufficient input from the corresponding control unit; assigning the fixed weight of 4 to the projections from the control

to the hidden units assured that, when maximum control was assigned to a task (i.e.,  $C_i = 1$ ), the corresponding hidden units were placed on the most sensitive range of their non-linear activation function (0.5)<sup>1</sup>. The activity of each hidden unit was related to its net input by the same logistic function as control units (see Eq. 3), with a gain parameter fixed to 1.

The hidden units projected their activity to the response units  $R$ , which represented the different responses (e.g., left and right button press) indexed by  $k \in \{1,2\}$ . The activity of response unit  $k$  was determined by the net input received from the hidden units:

$$net_k = \omega \cdot (H_{k,k} - H_{k,k^*} + H_{k^*,k} - H_{k^*,k^*}), k^* \neq k \quad (5)$$

where the input from hidden units was multiplied by connection weight  $\omega$  fixed to 1. The activity of each response unit was again related to its net input by the logistic function (see Eq. 3), with a gain parameter fixed to 1. We used the sign of the hidden unit inputs to the response units to implement the response congruence of stimulus features across tasks. For example, in the case of the parity and magnitude tasks, hidden units “odd” and “small”  $H_{1,1}$  and  $H_{2,1}$  provided excitatory (positive) input to the left response unit  $R_1$  and inhibitory (negative) input to the right response unit  $R_2$ , whereas the hidden units “even” and “large”  $H_{1,2}$  and  $H_{2,2}$  provided excitatory input to the right response unit  $R_2$  and inhibitory input to the left response unit  $R_1$ .

The response units provided input to a drift diffusion model (DDM) that implemented the decision process. This is a standard family of models for 2AFC decision making (e.g., (Bogacz

---

<sup>1</sup> See Cohen et al. (1990), pp. 338-9, for an interpretation of this implementation as a multiplicative effect of control through the summation of inputs passed through a non-linear processing function.

et al., 2006; Ratcliff, 1978) wherein noisy evidence favoring one alternative or the other is accumulated over time until a decision threshold  $z$  or  $-z$  is reached, at which point the corresponding response is selected and executed. The height of the decision threshold regulates the speed-accuracy trade-off, with low thresholds leading to faster and less accurate responses (i.e., lower response caution).

Within-trial changes in urgency were modeled as a progressive decrease in the decision threshold according to:

$$z_t = z_0 - t \cdot c \quad (6)$$

where  $z_0$  is the height of the decision threshold at the start of evidence accumulation,  $t$  is the timestep within a trial, and  $c$  is the collapse rate of the threshold. Thus, at higher values of  $c$  the threshold collapsed more quickly (reflecting higher urgency), leading to faster and less accurate responses; in contrast, when  $c$  was zero, the decision threshold remained fixed.

Evidence accumulation in the DDM began unbiased and proceeded according to:

$$dx = \frac{dt}{\tau} [R_1 - R_2 + \varepsilon], \quad x(0) = 0 \quad (7)$$

so that the drift rate ( $dx$ ) was determined by the difference in activation of the response units ( $R_i$ ) for a given time step ( $\tau$ ; fixed to 0.01) and subject to Gaussian distributed white noise ( $\varepsilon$ ; fixed mean = 0 and variance = 0.1). Once evidence accumulation started, the activity of the control units and the DDM decision process evolved synchronously with the same timestep parameter, so that post-stimulus changes in activation of the control units continuously propagated to the response units, and translated into a time-varying drift rate for the DDM.

Once a threshold was reached, the decision was recorded, and decision time was calculated as the number of timesteps taken until the threshold crossing multiplied by the timestep parameter  $\tau$ . RT was then calculated as decision time plus a non-decision time parameter ( $t_0$ ) that shifts the entire distribution of RT, for example to capture the duration of perceptual encoding and motor execution processes. Subsequently, the next trial began, with the control unit activities persisting across trials and the activity of all other units reset to 0.

### **Simulation of task performance**

We conducted simulations to examine how task-switching performance was impacted by gain on control signals, initial threshold, and collapse rate of the threshold. For each simulation, one of these parameters was varied while the others were held constant (see Table 1 for ranges and fixed values). For each set of parameters, we conducted 100 simulations of 1024 trials each, fixing task-switch frequency and response-incongruence frequency at 50%. Figure 3 plots the effect of these parameters on standard performance metrics (RT on correct trials, error rates (ER), and RR), separately for the four possible combinations of task-switch versus task-repeat and response-congruent versus response-incongruent trials. Figure 4 shows the effects on difference scores across conditions used to evaluate switch costs (task-switch minus task-repeat performance), which are traditionally taken as an inverse measure of flexibility, and incongruence costs (response-incongruent minus response-congruent performance), which are traditionally taken as an inverse measure of stability.

Control parameter	Value range when varied	Value when fixed
Gain	5 – 25	13
Threshold	0.01 – 0.10	0.07
Collapse rate ( $\times 10^3$ )	0 – 1.2	0

**Table 1.** Overview of control parameter values for simulation.

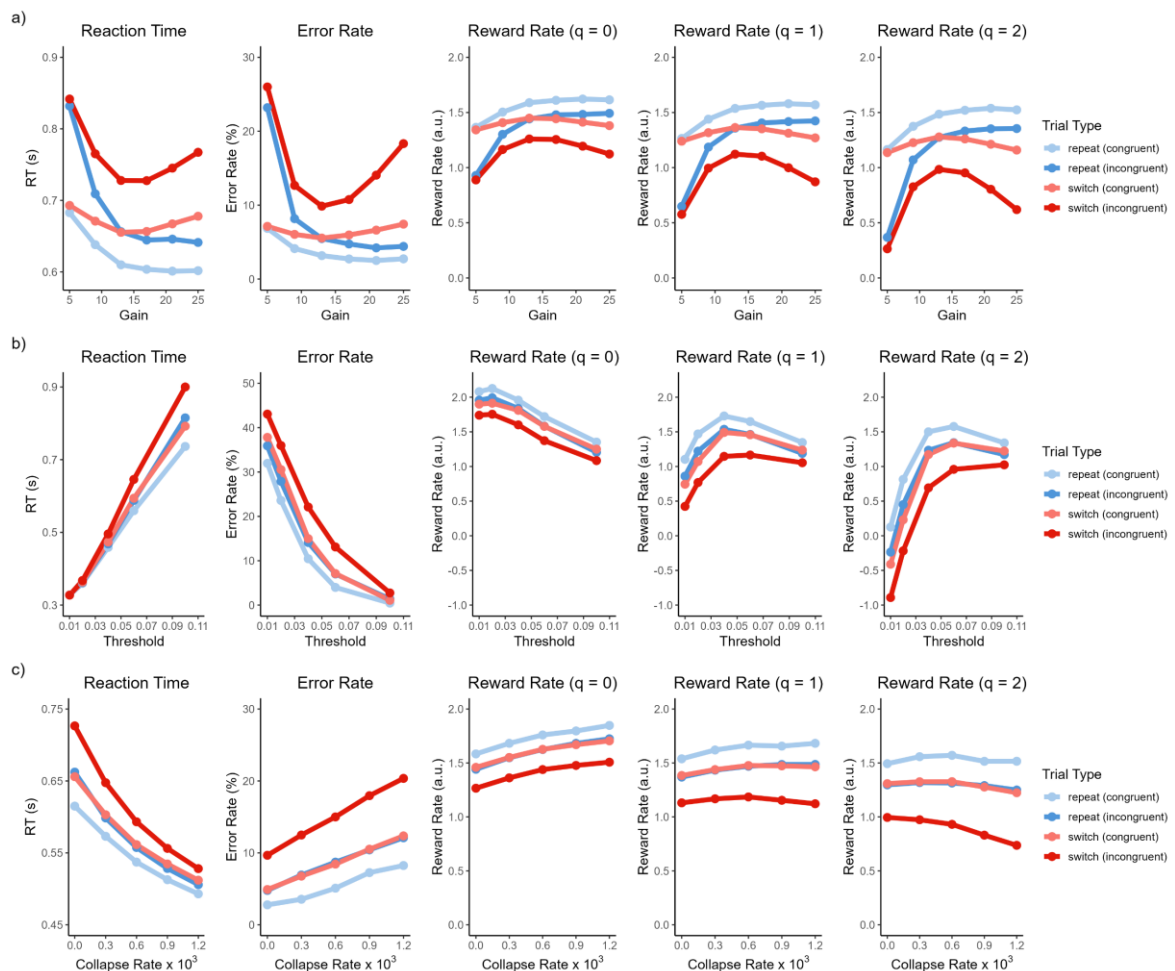


**Figure 3. Model simulations of task performance by trial type.** Task performance is simulated as a function of control intensity by varying the gain of the control units (a), as a function of response caution by varying the starting point of the DDM threshold (b), and as a function of within-trial urgency by varying the collapse rate of the DDM threshold (c). Colors indicate the trial types in the task-switching paradigm. Note that for each row, all model parameters were fixed except for the parameter on the x-axis. repeat = task-repeat, switch = task-repeat, congruent = response-congruent, incongruent = response-incongruent, a.u. = arbitrary units,  $q$  = error sensitivity.

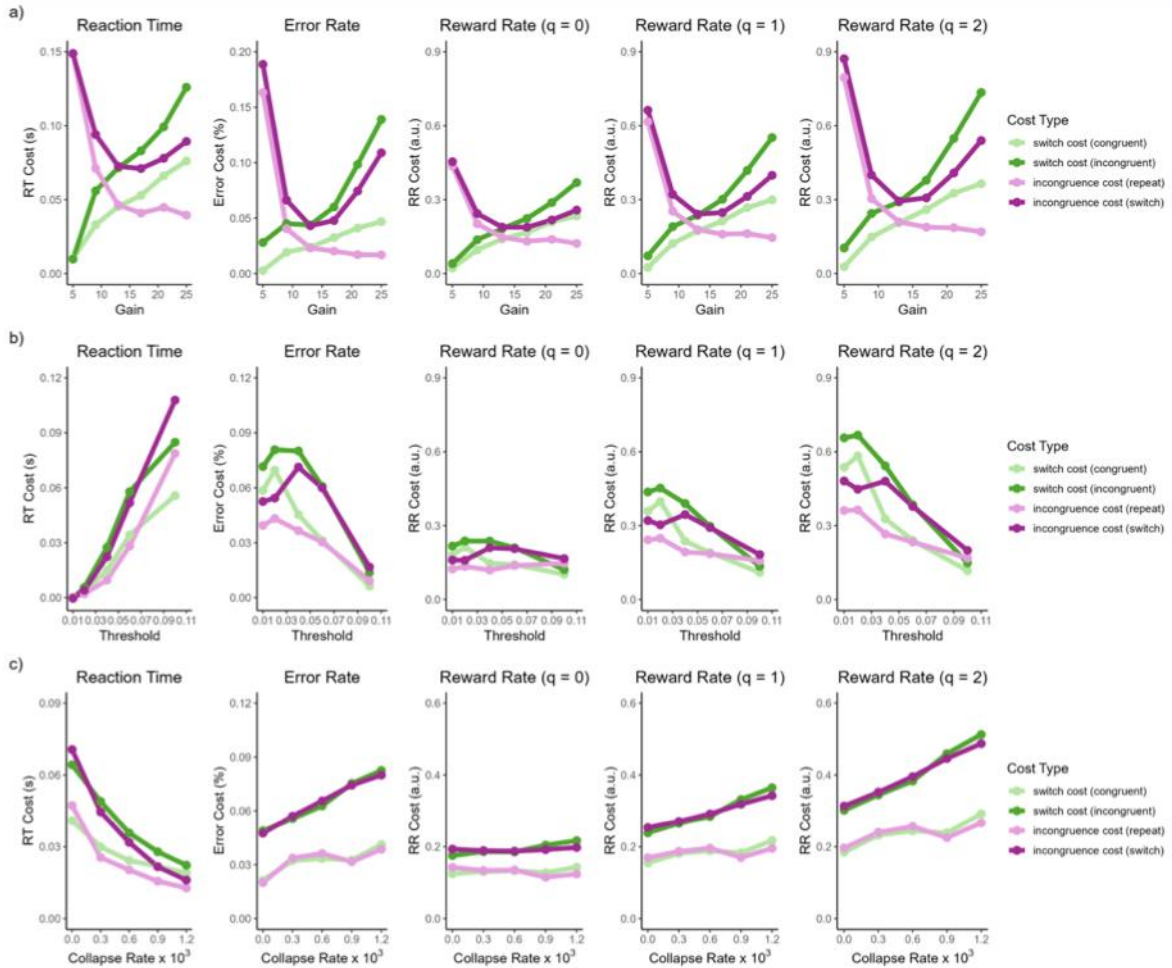


**Figure 4. Model simulations of task performance by difference score.** Task performance is simulated as a function of control intensity by varying the gain of the control units (a), as a function of response caution by varying the starting point of the DDM threshold (b), and as a function of urgency by varying the collapse rate of the DDM threshold (c). Colors indicate the performance difference scores in the task-switching paradigm. Note that for each row, all model parameters were fixed except for the parameter on the x-axis. repeat = task-repeat, switch = task-repeat, congruent = response-congruent, incongruent = response-incongruent, a.u. = arbitrary units, q = error sensitivity.

First, we examined the effects of varying gain on the control units while fixing decision threshold and collapse rate (Figure 3a, Figure 4a). The effect of gain on task-repeat trials was monotonic, with lower RT, lower ER, and higher RR at higher gain. In contrast, the effect on task-switch trials was non-monotonic, exhibiting an inverted U-shaped pattern that was especially pronounced on response-incongruent trials. In the lower range of gain (up to  $\sim 13$ ), increases in gain had a positive effect on performance for task-switch trials as it did for task-repeat trials. As we discuss below, this positive effect is related to the inclusion of a preparation

interval (i.e., a CSI) at the start of each trial. However, increases of gain beyond ~13 produced the expected decrease in performance on task-switch trials, consistent with its detrimental effect on flexibility. Because any positive effect of gain for task-switch trials was still weaker than for task-repeat trials, the switch cost increased monotonically with higher gain (Figure 4a, green lines). Importantly, this confirms that for a given set of task conditions, there is a level of gain that optimizes the trade-off between stability and flexibility.

Next, we examined the effects of varying the decision threshold while fixing the collapse rate and the control unit gain (Figure 3b, Figure 4b). As expected, lower thresholds led to lower RT and higher ER. These effects were larger on task-switch versus repeat trials and response-incongruent versus congruent trials. Consistent with previous work on RR optimization (Bogacz et al., 2006), the relationship between threshold and RR was non-monotonic, exhibiting an inverted-U-shaped pattern, with very low and very high thresholds producing suboptimal RR. Moreover, the RR-maximizing threshold was higher as sensitivity to errors increased. These findings reaffirm that there is an optimal trade-off between speed and accuracy that maximizes average RR.

Lastly, we examined the effects of varying the collapse rate of the decision threshold while fixing the starting point of the threshold and the control unit gain (Figure 3c, Figure 4c). In general, the effects of higher collapse rates resembled the effects of lowering a static threshold: higher rates of collapse led to faster RT, higher ER, and increases in RR, at least when sensitivity to errors was low. These findings indicate that a collapsing threshold can improve the RR.

Taken together, these simulations demonstrate several important points. Increases in gain monotonically improved performance on task-repeat trials, whereas the effect on task-switch trials was non-monotonic, with low and high gain impairing performance. These distinct effects of gain on performance can be understood in terms of the attractor dynamics in control unit

activation, and how gain determines the shape of the attractors associated with the prepared state for each task, which in turn influences the time required to transition between them. More specifically, increasing gain deepens the attractor associated with each control unit and increases the distance between them (Figure 2d, e). Deepening an attractor corresponds to greater activity of the corresponding control unit when it is fully prepared for the cued task (Figure 2c), in other words, strengthening the expression of the corresponding task representation. This improves performance on that task (e.g., reduces response-incongruence effects) by providing stronger “top down” support for processing in the corresponding pathway. However, at the same time, because of the increased depth of and distance between attractors, it takes longer to transition between them, thus increasing the switch cost. The impact of these attractor dynamics on switching performance is especially pronounced on response-incongruent trials. This is because on incongruent trials, if the control units have not fully settled into the correct prepared state, activity of the uncued task’s control unit leads to stronger processing of the uncued stimulus dimension, thereby activating the incorrect response which interferes with the correct one.

Similar dynamics of control were previously described by Musslick et al. (2019, 2018), who also showed that higher gain on control units led to increasingly longer transition times between attractor states (lower flexibility) and stronger activation of task-relevant representations (higher stability). Crucially, however, that previous work did not distinguish between task-switch and task-repeat trials when considering the effect of gain on incongruence costs<sup>2</sup>. As a result, they did not capture a key difference between these two types of trials, which we discuss next.

---

<sup>2</sup> See the supplementary materials of Jongkees et al. (2023) for an in-depth discussion of differences in the implementation and dynamics of control in Musslick et al. (2019, 2018) as compared to the model used in the present paper.

Our finding that high gain has a detrimental effect on task-switch, response-incongruent trials has novel implications for the interpretation of the incongruence cost as a measure of stability. Verbal theories often imply that an increase in stability monotonically reduces the average incongruence cost, reflecting a decrease in cross-task interference (Egner, 2023; Goschke & Bolte, 2014; Hommel, 2015). However, our simulations add an important caveat to this reasoning, which to the best of our knowledge has not yet been discussed in previous work, by demonstrating that high stability does not always reduce incongruence costs. Increases in gain did monotonically reduce incongruence costs on task-repeat trials, with the cost reaching a lower asymptote around a gain of 13 (Figure 4a, panels for RT and ER, pink lines). This asymptote occurred because the cued task control unit was nearing its highest possible activation while the uncued unit reached its lowest value (Figure 2c, dark and light red lines, respectively). The dynamics of task activation on task-switch trials were similar to those of task-repeat trials for the lower range of gain, with increasing gain leading to stronger activation of the cued and weaker activation of the uncued task (Figure 2c, dark and light green lines, respectively). This positive effect occurred because even though attractors are increasingly distant from each other at higher gain, with a sufficiently long CSI (in our simulations 0.5 s) it is still possible to reconfigure control sufficiently to be effective before the target stimulus appears.

Crucially, however, when gain exceeded ~15, the time required to transition between attractors became so long that the CSI did not provide enough time to adequately reconfigure control. As a result, the average activation of the cued task (post-CSI) decreased on task-switch trials and, conversely, average activation of the uncued task increased (Figure 2c). These dynamics produced a non-monotonic, inverted U-shaped change in the incongruence cost on task-switch trials (Figure 4a, purple lines). Importantly, this implies that an average of the incongruence cost across task-switch and repeat trials is not a clear indicator of stability, because an increase

in stability can reduce the average incongruence cost (in the lower range of gain) but also increase the average incongruence cost (in the higher range). As we demonstrate in the behavioral experiment reported below, some participants seem to adopt levels of gain in this higher range (approximately 15 up to 20). This presents a significant problem for the interpretation of the incongruence cost, because it is possible that even if all participants in a behavioral experiment increase their stability, the average incongruence cost might not change if there are individual differences in baseline stability. As the switch cost would still increase monotonically (Figure 4a), this pattern of results could mistakenly be interpreted as a change in flexibility without a corresponding change in stability.

An important implication of these observations is that care must be taken when defining and operationalizing stability and flexibility. Our simulations highlight that the switch cost and incongruence cost are not independent measures, because both are driven by performance on task-switch, response-incongruent trials. Consequently, an increase in gain beyond a certain point can produce increases in both costs. This is important because such a positive correlation between the two costs has been used as an argument against an obligatory trade-off between stability and flexibility (Egner, 2023; Mayr & Grätz, 2024). The reasoning is that a “one-dimensional” account requires that an increase in one cost is associated with a decrease in the other. To explain the empirical observation of a positively correlated change in the costs (Geddert & Egner, 2022, 2024), a “two-dimensional” account has been invoked that allows both stability and flexibility to increase or decrease at the same time. Our findings agree with this two-dimensional account, to the extent that stability and flexibility are strictly defined by these two behavioral measures. However, as outlined in the Introduction, here we formulate stability and flexibility not in terms of behavioral measures, which are the result of many interacting processes, some of which are unrelated to stability-flexibility (e.g., processes related to the speed-accuracy trade-off). Instead, we formulate stability and flexibility in terms of the

functional attributes of a processing system that can be regulated and optimized by control. Specifically, we define stability as the strength with which task representations are expressed in the system, and flexibility as the time required to fully transition between these tasks. From this perspective, stability and flexibility are two attributes of a system that are tightly coupled and in tension with each other, to the extent that tasks are incompatible due to overlap in processing demands and thus require mutual inhibition between them to manage interference. This definition of stability and flexibility in the context of incompatible tasks explicitly puts the two in tension while at the same time allowing that the switch and incongruence costs can jointly increase, as shown by our model simulations. Specifically, when task representations are strongly expressed in the system and the time required to transition between them is long (i.e., when gain is high), the average switch cost increases. At the same time, while transitioning between tasks, processing of the uncued stimulus dimension is elevated and thereby increases the incongruence cost. For this reason, the behavioral measures of switch and incongruence costs are not unambiguous indicators of stability and flexibility in terms of underlying mechanisms of control.

These nuances in the interpretation of behavioral measures apply even when participants do not adjust their control. Independent of contextual demands and corresponding shifts in performance, a trial-level (i.e., within-context) interaction between task transition and congruence is often taken as an indicator of the trade-off between stability and flexibility. Specifically, the finding that incongruence costs tend to be larger on task-switch than repeat trials is often taken as evidence that reconfiguration of control comes at a cost of momentarily increased interference (Kiesel et al., 2010; Meiran, 2000; Rogers & Monsell, 1995). However, this trial-level interaction is not consistently observed across studies and task conditions, which has been used as another argument against an obligatory trade-off between stability and flexibility (Egner, 2023; Mayr & Grätz, 2024). In contrast, our results indicate that the presence

or absence of this interaction in behavioral analyses can be explained at least in part by individual differences in gain and decision threshold. In the lower range of gain (i.e., when task representations are expressed weakly), the incongruence cost on task-switch and repeat trials is similar (Figure 4a) because activation of the uncued task is comparable on both types of trials (Figure 2c, up to gain ~13). Conversely, in the higher range of gain, the incongruence cost on task-switch and repeat trials diverges, as activation of the uncued task increases on switch trials and decreases on repeat trials (Figure 2c, beyond gain ~15). Additionally, the behavioral costs vary with threshold, converging in RT and diverging in ER at lower thresholds. This indicates that the trial-level interaction between task transition and congruence depends on the gain of participants, their threshold, and whether RT or ER are examined.

The above highlights that the interpretation of switch and incongruence costs is complicated by effects of the speed-accuracy trade-off. An increased emphasis on speed (lower threshold) can strongly impact RR, with more difficult trial types (task-switch trials and response-incongruent trials) being most affected (Figure 3b). This differential effect on trial types has major consequences for switch and incongruence costs, which decrease in RT and increase in ER with lower threshold (Figure 4b), further complicating their interpretation as measures of flexibility and stability.

To take comprehensive account of all the caveats and nuances raised above, research on the stability-flexibility trade-off requires mechanistic process models such as the one presented here, to assess latent variables of control (e.g., gain modulation of control signal intensity) that, while not observable directly in behavior, may nevertheless play a determining role in adjusting a trade-off between stability and flexibility. Specifically, the model we have described formalizes the effects that non-linear processing mechanisms, individual differences, and the confounding effects of the speed-accuracy trade-off may have in determining behavior.

### 3. Reward Rate Optimization of Control

In the preceding section, we described a model that provides a mechanistic account of how changes in control parameters can be used to regulate the trade-off between stability and flexibility, and the complex effects this can have on behavioral measures. Here, we focus on how the optimization of those control parameters, used to maximize average RR, can change, based on the contextual demand for flexibility.

#### Reward rate optimization

Specifically, we focus on manipulations of the frequency of task-switches, using the model to make normative predictions that we then test in a human behavioral experiment described in the next section. To do so, we generated trial sequences in which the task-switch frequency was either low or high, while response-incongruence frequency was fixed at 50% and counterbalanced between task-switch and repeat trials. Specifically, we simulated 35 sequences of 272 trials with 25% task-switches (“low-switch”) and 272 trials with 75% task-switches (“high-switch”), excluding a start-up trial (that cannot be categorized as switch or repeat).

We jointly optimized three model parameters to maximize average RR, separately for the two switch frequencies: gain on the control units, decision threshold, and the threshold collapse rate. Because it has not definitively been established whether a collapsing threshold improves RR (Boehm et al., 2020), we also conducted RR optimization with static thresholds by fixing the collapse rate to zero. Moreover, because optimal control parameters might be heavily influenced by sensitivity to errors, we compared optimizations with different error sensitivities ( $q$ ) in the RR calculation (*Equation 1*). Note that for consistency with the behavioral experiment, we considered simulated RTs above 1.5 s to exceed a response deadline and coded those trials as errors regardless of accuracy. As we discuss further below, this may have important implications for the optimality of within-trial urgency.

The model was simulated 10,000 times for each set of parameters and a given switch frequency, and model parameter values were identified that generated the highest average RR for that switch frequency. Parameter search was performed using the covariance matrix adaptation evolution strategy (CMA-ES) sampler from the Python package Optuna (3,000 iterations). We conducted parameter recovery tests to ensure identifiability of the parameters and found that recovery ranged from good to excellent (see Supplementary Materials).

### **Optimal parameters values**

*Gain.* Optimal gain was consistently lower when switch frequency was high, regardless of error sensitivity and whether the decision threshold was static or collapsing (Figure 5a). This is consistent with Musslick et al. (2019, 2018) and aligns with our own previous simulation results, where lower (but not too low) gain improved performance on task-switch trials. Importantly, this indicates that when task-switches are frequent, the improved switching at lower gain outweighs the increased interference between tasks, again showing that the optimal stability-flexibility trade-off depends on task conditions. Optimal gain at both switch frequencies increased with higher error sensitivities. This appears paradoxical because higher gain increases the likelihood of switch-related errors, but can be understood considering the joint increase in decision threshold, as discussed next.

*Threshold.* The optimal starting point of a static decision threshold (i.e., when the collapse rate was fixed to zero) increased with higher error sensitivity, shifting the emphasis to accuracy over speed (Figure 5b). This mitigates the likelihood of switch-related errors at higher gain. Moreover, high thresholds allow more time for reconfiguration of control *during* evidence accumulation, as captured in the model by a time-varying drift rate. This further reduces the impact of high gain on task-switch errors.

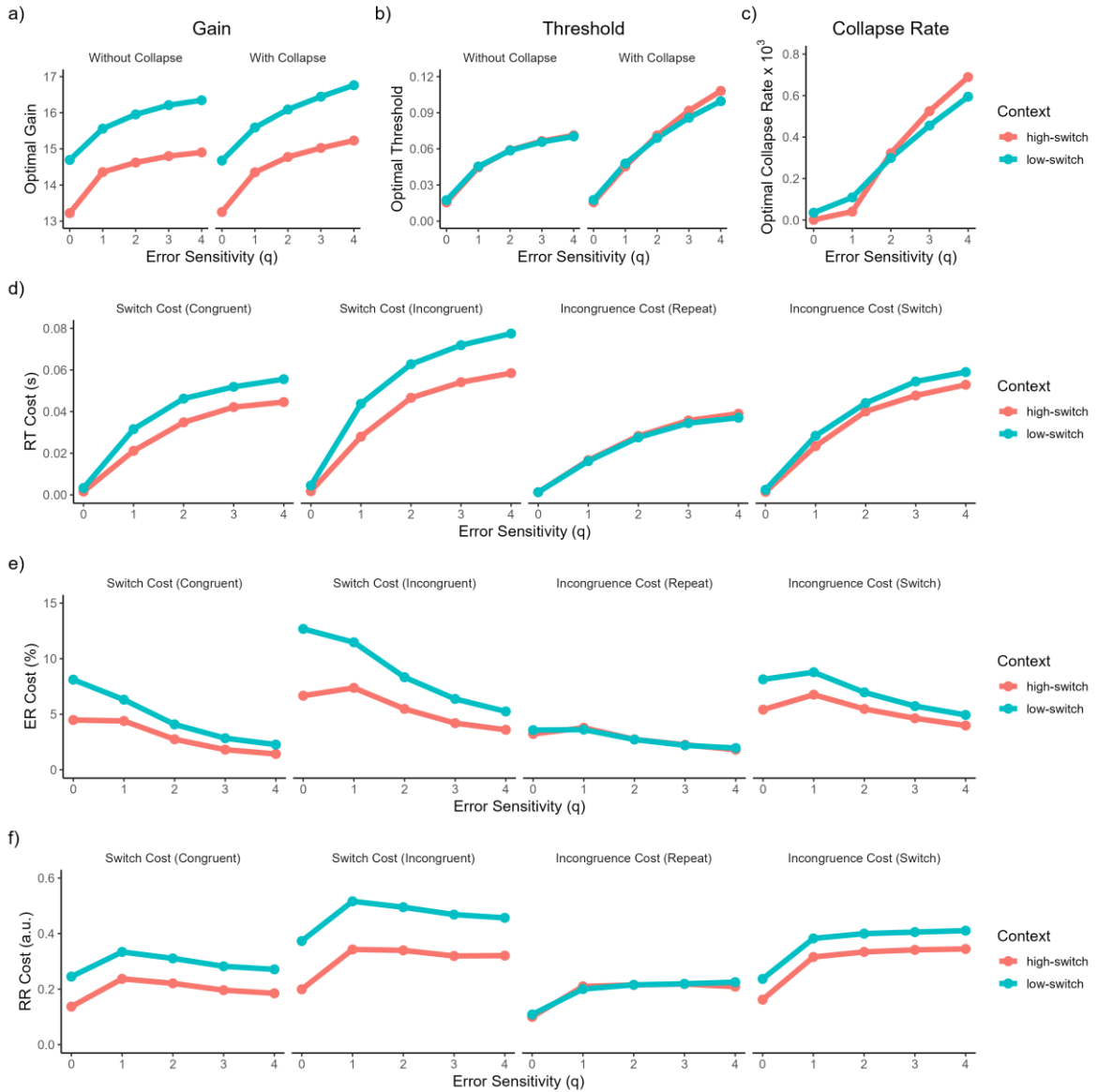


**Figure 5. Jointly optimized model parameters and corresponding performance costs.** Optimal gain (a), threshold (b), and threshold collapse rate (c) as a function of task-switch frequency context, error sensitivity and whether collapse rate was fixed to zero or not. Performance costs of the model with collapsing threshold, plotting correct RT (d), ER (e), and RR (f) as a function of task-switch frequency context and error sensitivity. repeat = task-repeat, switch = switch-repeat, congruent = response-congruent, incongruent = response-incongruent, a.u. = arbitrary units.

Notably, while the optimal starting point of a static decision threshold mostly overlapped for the two switch frequencies, the optimal starting point of a collapsing threshold diverged at the highest error sensitivities (Figure 5b), with the optimal starting point becoming higher for the high versus low switch frequency. This indicates that higher response caution was beneficial when demand for flexibility was high, but only when there was a strong emphasis on accuracy.

*Collapse rate.* Importantly, changes in the starting point of a collapsing decision threshold must be interpreted while considering the collapse rate. Overall, optimal collapse rate increased with higher sensitivity to errors, indicating that an increase in response caution at the start of a trial should be compensated by a stronger decrease in caution over the course of the trial (Figure 5c). This pattern is likely related to the inclusion of a response deadline in the RR calculation, where RTs exceeding 1.5 s were considered error trials (as in the behavioral experiment reported below). Specifically, with higher starting thresholds, the chance of missing the response deadline increased unless a compensatory increase in collapse rate curtailed very slow responses. Along these lines, where the starting point of the optimal high-switch threshold exceeded the low-switch threshold, so did the optimal collapse rate of the former exceed the latter. At the lowest error sensitivity ( $q = 0$ ), RR in the model with collapsing threshold was only 0.0023% higher than in the model with a static threshold. However, from  $q = 1$  to  $q = 4$ , this rose to 0.058%, 1.19%, 3.66%, and 7.19%, respectively, with the differences in RR being statistically significant for all 5 values of  $q$ ,  $p < 0.001$ . This indicates that a collapsing threshold can improve RR, especially as the chance of missing a response deadline increases.

### Predicted performance for optimized control parameters

*Analysis methods.* Next, we analyzed optimal task performance in the different switch-frequency conditions by simulating performance with the optimized control parameters, in order to generate predictions that could be tested in the behavioral experiment reported below. We did so by using the optimal parameters identified above in 100 simulations of the 35 trial sequences for each condition (high and low switch frequency), in order to capture the full range of RT distributions, average out simulation noise, and reliably detect even small changes in ER. Because the optimal parameters were quite similar between the models with and without collapsing decision threshold, we focus here on analysis of the model with a collapsing threshold.

Simulated performance was analyzed in R-Studio using the lme4 package for building and fitting linear mixed models (Bates et al., 2015). All mixed models are described using the R notation style.

We ran the following mixed model with random intercepts for each simulated trial sequence:

$$DV \sim switch-frequency * task-transition * congruence \quad (8)$$

where *DV* (dependent variable) was either correct RT, ER, or RR; *switch-frequency* denotes whether the trial belonged to the *high-switch* or *low-switch* condition; *task-transition* denotes whether the trial involved a *switch* or *repeat* trial; and *congruence* denotes whether the trial was response-congruent or response-incongruent. The interaction terms allowed us to examine whether the switch cost and incongruence cost differed between switch-frequency conditions. An interaction between switch and congruent trials was included to capture the possibility that incongruence costs may be larger on task-switch than repeat trials (Kiesel et al., 2010; Meiran, 2000; Rogers & Monsell, 1995), which would confound the interaction between switch frequency and incongruence costs if this were not included. That is, larger average incongruence costs in the high-switch condition could be observed simply because incongruence costs were larger on task-switch trials and those trials were more frequent. Moreover, a three-way interaction between switch frequency, switch and incongruent trials was included to capture whether changes in incongruence costs were different on task-switch and repeat trials. This was motivated by the simulation results indicating that beyond a certain level of gain, changes in the incongruence cost can be opposite on task-switch and repeat trials (Figure 4a).

Note that although mixed models are well-suited for single-trial analyses, analysis of RR requires averaging performance across trials. For consistency between the analyses of RT, ER, and RR presented here, each analysis was performed on averaged performance in every

combination of trial sequence, high-switch versus low-switch, task-switch versus repeat, and response-congruent versus incongruent trials.

*Results.* Plots of the predicted switch and incongruence costs (Figure 5d-e) showed a general trend in which, for optimal control parameters, increasing error sensitivity was associated with an increase in RT cost and a decrease in ER cost. Furthermore, these effects largely offset one another such that, for error sensitivities greater than 0, average RR remained relatively stable (Figure 5f). These effects on RT and ER costs were driven by the increasingly higher optimal decision threshold, consistent with our previous simulations (Figure 4b). As expected, switch costs were smaller in the high-switch condition, in line with the beneficial effect of lower gain on flexibility. Interestingly, the incongruence cost on task-repeat trials strongly overlapped between the switch-frequency conditions and was *higher* on task-switch trials in the low-switch condition.

At first glance, these effects may appear to violate a trade-off between stability and flexibility. However, close inspection of the optimal gain shows that, in the high-switch condition, even the lower gain was sufficiently high that it minimized the incongruence cost on task-repeat trials. This is because at gain values around 13, the control unit for the uncued task was near its lowest possible activation on task-repeat trials (Figure 2c). As a result, higher optimal gain in the low-switch condition was unable to produce further decreases in the incongruence cost on these trials. However, consistent with our previous simulations, the higher optimal gain in the low-switch condition did increase the incongruence cost on task-switch trials.

Taken together, the RR-optimization results broadly align with classic views on the stability-flexibility trade-off, but also provided some novel insights. On the one hand, optimal gain was lower when demand for flexibility was high, as determined by a high frequency of task-switches. This lower gain facilitated flexibility, as reflected in lower switch costs. However, the

gain was still high enough to minimize incongruence costs on task-repeat trials. As a result, the average incongruence cost on these trials did not differ between switch frequencies. On the other hand, the incongruence cost on task-switch trials was higher in the low-switch condition, consistent with the detrimental effect of high gain on task-switch, response-incongruent trials.

These results indicate that even in flexibility-demanding situations, there is a minimum level of stability that optimizes performance (in this case, minimizing the incongruence cost on task-repeat trials). Moreover, the results are consistent with our previous observations, showing that changes in switch and incongruence costs are not unambiguous indicators of changes in stability versus flexibility nor the extent of their interdependence. The average switch and incongruence costs were both higher in the low-switch condition, but rather than demonstrating stability-flexibility independence, these increased costs both reflected high stability. Importantly, this does not mean that participants in a behavioral experiment could never show decreased incongruence costs in low-switch conditions. Such a decrease could still be observed if their gain – that is, their level of stability – in the high-switch condition is suboptimal, and thus control unit activation of the uncued task is not yet minimized. As we report in the next section, this is indeed what we observed in our behavioral experiment.

#### 4. Empirical Testing of Normative Predictions

To test whether human performance conforms to the normative predictions of the model, we conducted a behavioral experiment in which participants switched between parity and magnitude tasks under conditions of low and high switch frequencies. We fit the model, using the same parameters used to optimize it for average RR, and examined the extent to which participants adjusted their control parameters as a function of the frequency manipulation, and the extent to which any such adjustments conformed to normative predictions described above. Furthermore, we used pupillometry and EEG to assess neurophysiological correlates of changes in control.

### Methods

#### Participants

Fifty individuals participated in return for a monetary compensation of €25,50 or course credits. They provided written informed consent, and the study was approved by the Psychology Research Ethics Committee of Leiden University. Three participants were excluded because of technical issues with the experimental software during one or both sessions. Twelve participants were excluded because they had an error rate of 30% or higher in one or more of the eight task conditions (each combination of switch frequency, task-switch/repeat and response-congruent/incongruent; see below). The remaining 35 participants (30 female), aged between 18 and 30 years, were included for further analysis. This sample is similar to group sizes in previous studies on task-switch frequency (Musslick et al., 2019) and uses a within-subjects design for increased statistical power.

#### Task

Participants completed a 2AFC task-switching experiment implemented using the Python package OpenSesame. On each trial, they had to indicate whether a target stimulus (numbers

1-4, 6-9) was smaller or larger than 5 (magnitude task) or whether it was odd or even (parity task), by pressing a key on a QWERTY keyboard: the "A" key with their left index finger for odd and smaller numbers and the numeric pad's "6" key with their right index finger for even and larger numbers. Participants were instructed to respond as quickly and accurately as possible. A task cue, presented briefly before the number appeared, indicated which task to perform. The cue was a colored circle (light green or blue, see below) or an outline shape (diamond or square; Figure 1). One of the outline shapes and one of the colors (randomly determined for each participant) indicated that the magnitude task should be performed, and the other outline shape and color indicated that the parity task should be performed. To deconfound the effects of task-switches and cue-switches (Monsell & Mizon, 2006), the cue changed on every trial, alternating between shape and color. Trials on which the number was associated with the same response key in both tasks (1, 3, 6, 8) were classified as response-congruent; trials on which the number was associated with different keys in the two tasks (2, 4, 7, 9) were classified as incongruent. The interval between each response and the subsequent task cue (RCI) was fixed at 3 s. This fixed RCI ensured that pupils had sufficient time to return to baseline levels, regardless of response speed. If a participant failed to respond within 1.5 s, the trial was registered as incorrect, and the inter-trial interval (ITI) time (1.5 s) for the next trial started.

Participants completed two sessions on different days spaced 5 to 9 days apart. Each session consisted of 28 blocks of 17 trials. In the first 20 blocks, switch frequency was manipulated: one session had blocks with 75% task-switch trials (*high-switch* condition), and the other had blocks with 25% task-switch trials (*low-switch* condition). The trial sequences in these blocks were based on those used for RR optimization, to facilitate comparison between the RR-maximizing control parameter values reported in the previous section and the parameter values adopted by participants. The order of the two sessions was counterbalanced across participants. In both sessions, task-switch and repeat trials each involved 50% response-congruent and 50%

incongruent numbers. The CSI was kept constant at 0.5 s. In the final eight blocks of each session, the switch frequency was set to 50%. During these blocks, CSI was varied across trials: half of the trials had a CSI of 0.5 s, and the other half had a CSI of 1.2 s. The longer CSI allowed us to investigate cue-evoked EEG responses without interference from the next stimulus. However, because we did not replicate previous findings of cue-evoked alpha-band oscillations (Siqi-Liu et al., 2022), we do not report data from these variable-CSI blocks.

At the start of each session, participants completed a set of practice blocks: one block of 17 trials of the magnitude task, one block of the parity task, and four blocks of task switching with 50% task-switch trials. In these practice blocks, participants received trial-by-trial feedback on their performance at the end of each trial. Participants had to achieve at least 75% accuracy in each block to proceed to the main experiment. During the main experiment, participants were shown their average accuracy and RT after each block.

### **Behavioral analyses**

Before statistical analysis, we discarded the first three blocks (to allow adjustment to the switch-frequency condition) and the last eight blocks (to remove the variable-CSI blocks). Additionally, we excluded the first two trials of each block and all post-error trials, which may involve adjustment of control in a way that we do not consider here. For the RT analysis, the data were then split by participant, switch-frequency condition, task transition, and congruence, and we removed trials with RT exceeding 2.5 standard deviations from the cell mean. This last outlier removal step led to the exclusion of 2.7% of the trials.

We conducted single-trial statistical analyses in R-Studio using the lme4 package for building and fitting linear mixed models (Bates et al., 2015). The independent variables were z-scored by participant. The dependent variables were z-scored over all participants because the mixed models were designed to consider between-subject differences in these variables; each model

included a random intercept for each participant. We ran the models described below, and report results excluding nonsignificant regressors to increase precision. A complete overview of all statistics for each predictor is presented in the Supplementary Materials.

First, we analyzed RTs using the following mixed model:

$$RT \sim switch-frequency + congruence + task-transition + digit + \\ task-transition_{prev\_trial} + task-transition_{prev\_trial}:task-transition + \\ switch-frequency:task-transition + switch-frequency:congruence + \\ congruence:task-transition \quad (9)$$

where *switch-frequency* denotes whether the trial belonged to the *low-switch* or *high-switch* condition, *congruence* denotes whether the trial was congruent or incongruent, *digit* denotes the digit shown, *task-transition* denotes whether the trial was a switch or repeat trial, and *task-transition<sub>prev\_trial</sub>* denotes whether the previous trial was a switch or repeat trial. We used the interaction terms with *switch-frequency* to test the key hypothesis that the switch costs and incongruence costs differed between switch-frequency conditions. Note that the inclusion of *task-transition<sub>prev\_trial</sub>* ensured that any “global” (i.e., contextual) effects of switch frequency on switch costs were deconfounded from more “local” (i.e., trial-to-trial) effects of consecutive switch trials on switch costs (Brown et al., 2007; Mayr & Keele, 2000). Moreover, the inclusion of an interaction between *task-transition* and *congruence* ensured that any effects of switch frequency on incongruence costs were deconfounded from the finding that incongruence costs tend to be larger on switch trials (Kiesel et al., 2010; Meiran, 2000; Rogers & Monsell, 1995).

Next, we analyzed ER using the same mixed model:

$$error \sim switch-frequency + congruence + task-transition + digit + \\ task-transition_{prev\_trial} + task-transition_{prev\_trial}:task-transition + \\ switch-frequency:task-transition + switch-frequency:congruence + \\ congruence:task-transition \quad (10)$$

where *error* is a binary variable denoting whether the response was incorrect. Since the error variable is binary, we ran a mixed model with a binomial distribution (all other models used the standard Gaussian distribution).

### **Computational modeling of behavior**

We fit the process model to behavioral data using an approximated maximum likelihood estimation method (Turner & Sederberg, 2014). Each participant was fit individually by simulating the model 10,000 times for each proposed set of parameter values, applying probability density estimation to the simulation results to approximate the likelihood function, and using an optimization algorithm to minimize the negative log-likelihood, in our case the CMA-ES sampler from the Python package Optuna (5,000 iterations). The free parameters (Table 2) were gain on the control units, decision threshold, collapse rate of the threshold, and non-decision time. Although non-decision time was not a focus of our investigation, we nevertheless fit the parameter to capture individual differences in RT. Each parameter was allowed to vary by switch-frequency condition.

Note that model fits used the same data as the behavioral analysis (i.e., after trial exclusions; see above). Importantly, however, because the dynamics of model unit activations rely heavily on the exact sequence of trials, the trials excluded for analysis were nevertheless simulated in their proper place, but not considered in optimization of the likelihood.

<i>Parameter</i>	<i>Lower bound</i>	<i>Upper bound</i>	<i>Granularity</i>
Gain	5	20	0.1
Threshold	0.03	0.15	0.0005
Collapse rate ( $\times 10^3$ )	0	3	0.01
Non-decision time (s)	0.2	0.5	0.001

**Table 2.** Overview of free parameters. Granularity indicates the absolute size of spacing between possible parameter values.

The resulting parameter estimates were z-scored across all participants and switch frequencies and analyzed with the following mixed model with random intercepts for each participant:

$$DV \sim \text{switch-frequency} + \text{session}_{nr} + \text{switch-frequency: session}_{nr} \quad (11)$$

where  $DV$  was either control unit gain, decision threshold, collapse rate of the threshold, or non-decision time.

For the fits described above, control parameters were only allowed to vary by switch frequency and not also from trial-to-trial *within* each frequency condition. In an attempt to fit such within-condition changes in control as informed and constrained by neurophysiological data, we also examined the extent to which variations in pupil size and EEG posterior alpha power (see below) were associated with trial-to-trial changes in control parameters within each condition. For this purpose, we also jointly fit these measures along with behavior and examined whether this provided a superior fit to the data. To do so, we computed the trial-to-trial time series for each control parameter as:

$$b_n = b_{base} + \theta \cdot \alpha_n \quad (12)$$

where  $b_{base}$  is an intercept value of the model parameter,  $\alpha_n$  is the neurophysiological measurement on trial  $n$  (e.g., single-trial baseline pupil size, see below), and  $\theta$  is a multiplicative weight that scales the relationship between the neurophysiological data and model parameter. To limit the impact of noise in the neurophysiological measurements, we quantized the single-trial measure ( $\alpha$ ) into 5 bins, separately for each participant and switch frequency condition, and mean-centered the resulting variable. Thus, for each participant and trial,  $\alpha_n$  could take the value -2, -1, 0, 1, or 2. We compared BIC scores of models for which  $\theta$  was fixed to zero to those for which  $\theta$  was fit separately per switch-frequency condition. Note that for these model fits, in addition to the trial exclusions reported above, we additionally excluded trials with missing neurophysiological data from the likelihood optimization (as described for each measure below). Moreover, based on prior model comparisons (reported in the Results) we constrained the intercept value for the threshold collapse rate to be the same across switch frequencies, while allowing  $\theta$  to vary. None of the model comparisons favored models with trial-by-trial variation in control parameters as a function of the neurophysiological measures. This might indicate that trial-by-trial changes in these measures were too noisy to be reliably related to trial-by-trial changes in control parameters, or that our design was statistically underpowered to detect subtle effects. For this reason, in the Results section we report the models without joint fitting of trial-by-trial behavior and neurophysiology and restrict our analysis of the neurophysiological data below to comparisons across conditions.

## Pupilometry

To minimize luminance-related pupil-size changes, we used isoluminant Teufel colors for the task cues and background. The color cues were light green (RGB 126, 191, 77) and slate blue

(RGB 123, 178, 208), and were displayed on a purple background (RGB 166, 160, 198). The fixation cross, outline shape cues and numbers were black. Pupil diameter was recorded using a Tobii-Pro eye tracker at a 40-Hz sampling rate under ambient light of 7.2 cd/m<sup>2</sup>. Before the main experiment, the eye tracker was calibrated. During calibration and the main experiment, participants rested their heads on a chin rest positioned 75 cm from the screen.

Three participants were excluded from analyses of pupil size due to technical issues with the eye tracker during recording. Pupil data from thirty-two participants were preprocessed using functions from the gazer package, custom-made functions in R, and the BPR toolbox in MATLAB (Yoo et al., 2021). Blinks were identified using the blink detection method of Yoo et al. (2021). Individual blink-locked pupillary responses were fitted and regressed out to remove blink effects from the pupil data, also as described by Yoo et al. (2021). Six participants were excluded from further analysis due to insufficient intact blinks for model fitting or poor blink fits, leaving data from 26 participants.

Trials with over 40% missing samples during the baseline period (-0.6 to -0.5 s relative to stimulus onset) or the trial period (-0.5 to 2 s relative to stimulus onset) were discarded (0.3% of trials). After blink preprocessing, the remaining missing data were filled using linear interpolation, and the data were smoothed with a moving-average filter (width of 10 samples). Artifacts were identified and removed using the *max\_pupil\_dilation* function from the gazer package, implementing the outlier detection formula by Kret and Shak-Shie (2019) (5.4% of trials). Finally, trials on which the baseline pupil size deviated from the mean by more than two standard deviations were removed (Mathôt & Vilotijević, 2022) (3.7% of trials).

To identify time periods during which baseline pupil size differed between switch-frequency conditions, we binned pupil size in 0.05 s bins from 1.2 s to 0.5 s before stimulus onset, and ran the following mixed model per bin:

$$\text{BaselinePupil} \sim \text{switch-frequency} + \text{session}_{nr} + \text{PeakPupil}_{prev} + \\ \text{block} + \text{block}^2 + \text{blocktrial} + \text{blocktrial}^2 \quad (13)$$

where *BaselinePupil* denotes the average pupil size within that bin, *session<sub>nr</sub>* denotes whether it was the first or second session, *PeakPupil<sub>prev</sub>* denotes the maximum pupil dilation on the previous trial (which could potentially spill over into the subsequent ITI), *block* denotes the block number, and *blocktrial* denotes the trial number within each block. We added the exponentials of *block* and *blocktrial* to capture potential non-linear time-on-task effects on pupil size. To control for multiple comparisons, we employed a cluster-based permutation analysis with 1000 permutations. Specifically, we shuffled the *switch-frequency* regressor and calculated the size of significant clusters of time points in each shuffled dataset. We then compared the size of these clusters with those observed in the actual data. Clusters of significant time points were considered statistically significant if they fell at or beyond the 0.05 threshold of the permutation distribution.

To examine the effect of switch frequency on evoked pupil dilations, we ran the following mixed model:

$$\text{PeakPupil} \sim \text{switch-frequency} + \text{session}_{nr} + \text{BaselinePupil} + \text{task-transition} + \\ \text{congruence} + \text{cue}_{shown} + \text{block} + \text{block}^2 + \text{blocktrial} + \text{blocktrial}^2 \quad (14)$$

where *PeakPupil* is the maximum pupil dilation on each trial, and *cue<sub>shown</sub>* indicates the specific combination of the color and shape of the cue.

### **EEG data collection and processing**

Continuous EEG data were acquired using an ActiveTwo system (<http://biosemi.com>) from 64 scalp electrodes, configured to the standard 10/20 setup, and digitized at 512 Hz. Electrodes placed on the mastoids served as reference points.

We preprocessed the EEG data of 35 participants using a combination of manual and automatic preprocessing steps using the Python package MNE. First, we checked for electrode bridging. If bridging was present, we interpolated the electrodes. Next, we low-pass filtered the data at 0.5 Hz and divided the data into epochs from 3.5 to 2 s before stimulus onset. The wide time range prevented edge artifacts in the time-frequency decomposition described below. We then used the *autoreject* algorithm to automate unified rejection and repair of bad epochs (Jas et al., 2017), by identifying bad epochs using a first-pass *autoreject*, and then filtering out those epochs. This filter significantly increased the quality of subsequent calculation of ICA components. After manual component rejection (mainly focused on eye-blink artifacts and other artifacts in the signal that we could clearly distinguish from brain activity), we filtered out these components and re-ran the *autoreject* algorithm over all epochs, including trials excluded from the ICA. We rejected participants when more than 50% of their trials were rejected in one or both sessions, which led to the removal of 2 participants from analyses of EEG data, leaving data from 33 participants for further analysis.

### **EEG time-frequency analysis**

For the time-frequency analysis, we followed the procedure by Siqi-Liu et al. (2022), implemented using the Python package MNE (Gramfort et al., 2013). We decomposed the EEG time series into time-frequency representations using a multitaper method, estimating power with discrete prolate Slepian sequences at logarithmically spaced frequencies from 2 to 30 Hz in 30 steps. The Gaussian width of the multitapers was set based on frequency: two cycles for frequencies < 4 Hz, three cycles for frequencies < 7 Hz, five cycles for frequencies < 14 Hz, and seven cycles for higher frequencies. These settings provided a good balance between temporal and frequency resolution. The time-bandwidth product was set at four. Before calculating power, we computed the event-related potentials on task-switch and repeat trials for each switch-frequency condition, and removed those from the epoch data.

For the alpha power analyses, we focused on parieto-occipital electrodes, following prior research (Liu & Yeung, 2020; Siqi-Liu et al., 2022). Accordingly, we isolated the frequency band between 8 and 14 Hz and averaged data from the electrodes Pz, POz, Oz, P1, P2, PO3, PO4, O1, and O2. To identify time periods during which posterior alpha power differed between switch-frequency conditions, we divided each epoch into 0.05 s time bins from -1.5 until 2 s relative to stimulus onset and estimated the following mixed model for each bin:

$$\text{precue alpha power} \sim \text{switch-frequency} + \text{session}_{nr} + \text{block} + \text{block}^2 + \text{blocktrial} + \text{blocktrial}^2 \quad (15)$$

The purpose of this analysis was to identify whether, and within which time range, parieto-occipital alpha power differed significantly between switch-frequency conditions, as well as the direction of these differences. To account for multiple comparisons, we again ran a cluster-based permutation analysis with 1000 permutations.

Finally, we tested whether baseline pupil size and precue alpha power were correlated across trials. To do so, we ran the following mixed model on the residuals, obtained after regressing out the independent variables (except switch frequency) in *Equations 13 and 15* (see Supplementary Materials).:

$$\text{precue alpha power} \sim \text{BaselinePupil} + \text{BaselinePupil}^2 + \text{switch-frequency} + \text{BaselinePupil: switch-frequency} + \text{BaselinePupil}^2: \text{switch-frequency} \quad (16)$$

As a single-trial measure of baseline pupil size, we took the average pupil size from 1.2 to 0.85 s before stimulus onset, the interval during which the effect of switch frequency was significant. As a single-trial measure of precue alpha power, we calculated the average alpha power from -1.5 to -1 s relative to stimulus onset, a part of the window during which the effect of switch frequency was significant (see *Results*). This period was chosen as it was 0.5 s after the stimulus

offset of the previous trial and 0.5 s before the cue onset of the next trial, providing a clean between-trial measure of alpha power.

## Results

### Adaptation of switch costs and incongruence costs

Mean correct RT (Figure 6a,b) showed the predicted effects of task transition, congruence, and their interactions with switch frequency: RTs were slower on task-switch trials than on task-repeat trials (*Equation 9*:  $\beta = -0.08$ , 95% CI [-0.10, -0.07],  $t(14850) = -9.50$ ,  $p < .001$ ) and slower on incongruent trials than on congruent trials ( $\beta = 0.19$ , 95% CI [0.15, 0.23],  $t(14850) = 9.37$ ,  $p < .001$ ). Importantly, these effects were modulated by switch frequency. In the *low-switch* condition there was an increased switch cost ( $\beta = 0.05$ , 95% CI [0.03, 0.07],  $t(14850) = 5.33$ ,  $p < .001$ ), and a trend effect towards decreased incongruence costs ( $\beta = -0.02$ , 95% CI [-0.00, 0.03],  $t(14850) = 1.90$ ,  $p = .058$ ) compared to the *high-switch* condition (Figure 6c). These results match the model predictions of optimal performance as a function of switch frequency (Figure 5d), demonstrating a reduction of switch costs when switches were frequent.

The main effects in error rates mirrored the RT results (Figure 6a,b): Error rates were larger on task-switch trials than on repeat trials (*Equation 10*:  $\beta = -0.16$ , 95% CI [-0.23, -0.09],  $z = -4.73$ ,  $p < .001$ ), and larger on incongruent trials than on congruent trials ( $\beta = -0.42$ , 95% CI [-0.49, -0.36],  $z = -13.57$ ,  $p < .001$ ). There was a larger incongruence cost in the low-switch condition than in the high-switch condition (Figure 6c;  $\beta = 0.07$ , 95% CI [0.01, 0.14],  $z = 2.18$ ,  $p = .03$ ), which appears to be driven by lower congruent ERs in the low-switch condition rather than high incongruent ERs. Conversely, there was no significant difference in switch costs ( $\beta = 0.04$ , 95% CI [-0.03, 0.12],  $z = 1.13$ ,  $p = .26$ ).

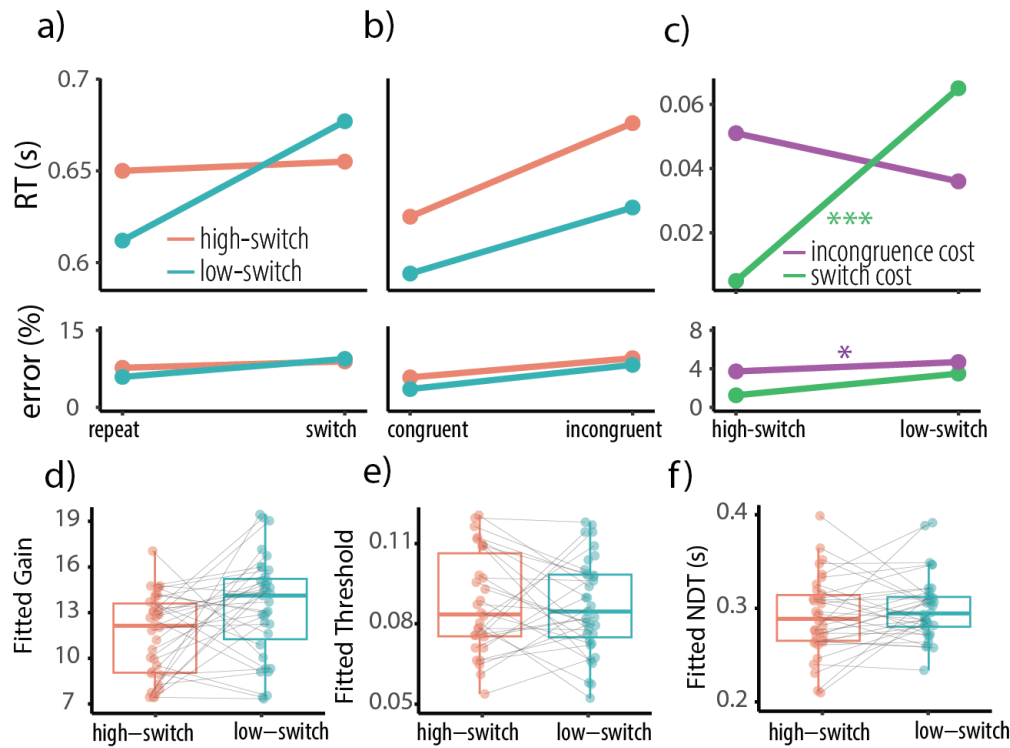


**Figure 6. Behavioral results.** a) Mean correct response times and error rates as a function of switch frequency and task transition, or b) congruence. c) Switch costs and incongruence costs, separately for each switch-frequency condition. d), e), f) Fitted parameters per switch frequency. NDT = non-decision time.  $p < .05$ : \*;  $p < .01$ : \*\*;  $p < .001$ : \*\*\*, derived from Equation 9/10.

#### Adaptation of control parameters

Because prior work indicates that participants do not always exhibit within-trial urgency, we first fit collapse rate of the decision threshold individually for each participant and switch frequency, and compared the results with fits in which collapse rate was estimated either per participant but constrained to be the same for both frequencies, or fixed to zero. Model comparison indicated that the model with a single collapse rate for both switch frequencies provided the best fit for most participants, as indicated by lower BIC scores (23 out of 35 participants favored the model with a single collapse rate, 3 participants favored the model with separate collapse rates, and 9 participants favored the model without collapsing threshold). Notably, the models with a collapsing threshold better captured the right tail of the RT distributions – those RTs closest to the response deadline (see Supplementary Materials for posterior predictive checks). In contrast, the model with static thresholds produced RTs that

were too slow, particularly in the right tail. Since the model with the same collapse rate for both switch frequencies provided the best fit for most participants, below we focus on this model when reporting the results for other parameter estimates (a complete overview of all statistics for each predictor in Equation 11 is presented in the Supplementary Materials).

Participants broadly adhered to the normative predictions described in the previous section: there was a significant effect of task-switch frequency on gain of the control units, with lower gain when switch frequency was high,  $F(33) = 7.31, p = 0.010$  (Figure 6d). This indicates, consistent with previous work (Musslick et al., 2018, 2019), that participants indeed adopted a lower intensity of control signals, trading flexible switching for increased cross-task interference. Model-fitted gain did not vary by session number,  $F(33) = 0.76, p = 0.390$ , nor was there a significant interaction between switch frequency and session number,  $F(33) = 2.31, p = 0.138$ . This indicates that adaptation of control signal intensity was comparable in the first and second session of the experiment.

In contrast, the model-fitted starting point of a collapsing decision threshold only showed a significant effect of session number, with lower decision thresholds in the second session,  $F(33) = 18.54, p < 0.001$  (Figure 6e). Taken together with the fact that the best-fitting model included a single threshold collapse rate for both frequencies, these results indicate that participants did not adjust their response caution or within-trial urgency to task-switch frequency. This is broadly in line with our simulation results indicating that optimal thresholds and collapse rates for the two frequencies only diverge at very high levels of error sensitivity; and, even then, afford only a relatively small increase in overall RR.

Analysis of non-decision time indicated no significant effects of switch frequency, session number, nor an interaction between the two (all  $p > 0.285$ ), indicating that participants did not adjust their non-decision time (Figure 6f).

Taken together, these model-fitting results indicate that participants conformed to the normative predictions of the model. To examine how close the empirically fit control parameters of the model were to optimal, we related the parameter estimates to the RR-optimized parameters using the same trial sequences, as described in the previous section. Average participant gain in the high-switch condition was 11.6 (range 7.7 to 16.9), which is below the level of gain that minimized activation of the uncued task on task-repeat trials (Figure 2c) and thereby minimizes the incongruence cost (Figure 4a). At the same time, the average participant gain in the low-switch condition was 13.4 (range 7.6 to 19.2), which is remarkably close to the optimal gain that minimized the incongruence cost. Nevertheless, the mean gain in both conditions was below optimal (RR-maximizing) values (cf. Figure 5a), suggesting that on average participants overemphasized flexibility.

The finding that participants adopted suboptimal gain in the high-switch condition is consistent with the trend we observed in the behavioral results. That is, the average high-switch gain was low enough (i.e., lower than 13) that a modest increase in gain in the low-switch condition could produce a decrease in control unit activation of the uncued task (Figure 2c), leading to smaller incongruence costs in the low-switch condition. However, large individual differences in high-switch gain mean that this did not apply to all participants. As a result, the average of the sample reflected only a marginal difference in incongruence costs between the frequencies, whereas analysis of latent variables (i.e., control unit gain) more clearly revealed adaptation of control.

The average model-fitted decision threshold was 0.085 (range 0.046 to 0.127), which roughly corresponds to the optimal threshold when error sensitivity ( $q$ ) is 3 (Figure 5b). This suggests that participants did not strictly maximize RR but instead prioritized a combination of RR and accuracy. However, large individual differences in threshold indicate that some participants were more RR-optimal than others. Notably, and consistent with prior work on practice effects (Balci et al., 2011), the average threshold decreased from 0.092 (range 0.056 to 0.125) in the

first session to 0.078 (range 0.046 to 0.127) in the second session. This suggests that participants learned to adopt lower, more RR-optimal thresholds over time. Moreover, the average model-fitted threshold collapse rate ( $\times 10^3$ ) was 0.476 (range 0.050 to 0.880), which is roughly the optimal collapse rate for their average threshold (Figure 5c). Taken together, this suggests that participants were generally overly cautious in responding but, given their thresholds, the level of within-trial urgency was close to optimal for maximizing average RR.

### **Higher switch frequency is associated with larger baseline pupil size and evoked pupil dilations**

Each session began with a block of 34 trials in which participants passively viewed the task stimuli used in the actual experiment. This block allowed us to examine the pupillary light reflex associated with the stimuli in the absence of task-related pupil changes. Despite our efforts to minimize stimulus-related luminance changes by using isoluminant colors, small pupillary responses to task cues remained, especially between shape and color cues, which led us to include a task-cue regressor in our mixed model predicting maximum pupil dilation (*Equation 14*). We also accounted for eye-blink effects in the pupil data (Knapen et al., 2016) by regressing out blink effects (Yoo et al., 2021) before analyzing the pupil time series data.

Bin-wise mixed model analyses showed a significant difference between switch-frequency conditions in baseline pupil size from 1.2 to 0.85 s before stimulus onset, with larger pupil sizes in the high-switch condition (Figure 7a,b; *Equation 13*). Additionally, we found a significant difference between switch-frequency conditions in maximum pupil dilation (Figure 7c,d; *Equation 14*:  $\beta = 0.03$ , 95% CI [0.01, 0.05],  $t(11430) = 2.99$ ,  $p < .01$ ). Specifically, the high-switch condition was associated with larger maximum pupil dilation. These relationships between switch frequency and pupil-linked arousal measures could provide important clues about the mechanisms underlying control adaptation to the contextual demand for cognitive flexibility, that we consider in the *Discussion*.

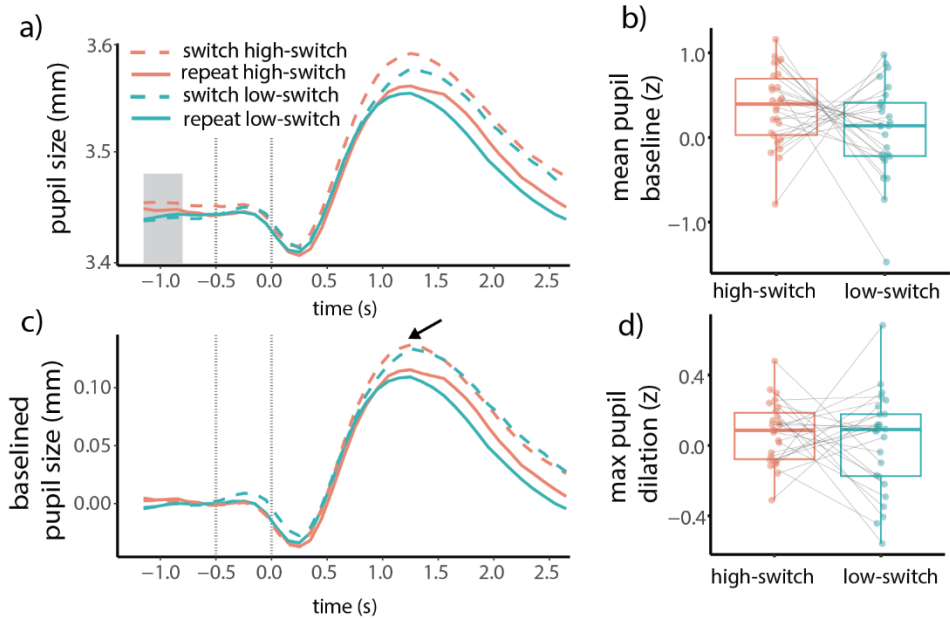


**Figure 7. Switch frequency modulates pupil size measures.** a) Average pupil waveforms for each condition. The grey dotted lines indicate cue onset and stimulus onset. The grey box indicates the time period during which pupil size differed between the high- and low-switch conditions. b) Average baseline pupil size during the marked time period for each participant and switch frequency. c) Average baseline-corrected pupil waveforms. The arrow indicates the maximum pupil dilation that was computed for each condition. d) Average maximum pupil dilation during the marked time period for each participant and switch frequency. Black lines show the average switch-frequency effects on the two pupil size measures. Note that at the level of individual participants the effect of switch frequency is confounded by session effects (e.g., a practice effect).

### Higher switch frequency is associated with larger baseline alpha power

Previous research has found effects of switch frequency on posterior alpha power (Liu & Yeung, 2020; Siqi-Liu et al., 2022), that we sought to replicate here by analyzing differences in posterior alpha power between the high-switch and the low-switch condition. Bin-wise mixed model analyses exploring the entire epoch (-1.5 to 2.5 s) indicated that alpha power was significantly stronger in the high-switch condition from -1.5 to 0.5 s and from 1.0 to 2.5 s relative to stimulus onset (Figure 8a,b; *Equation 15*).

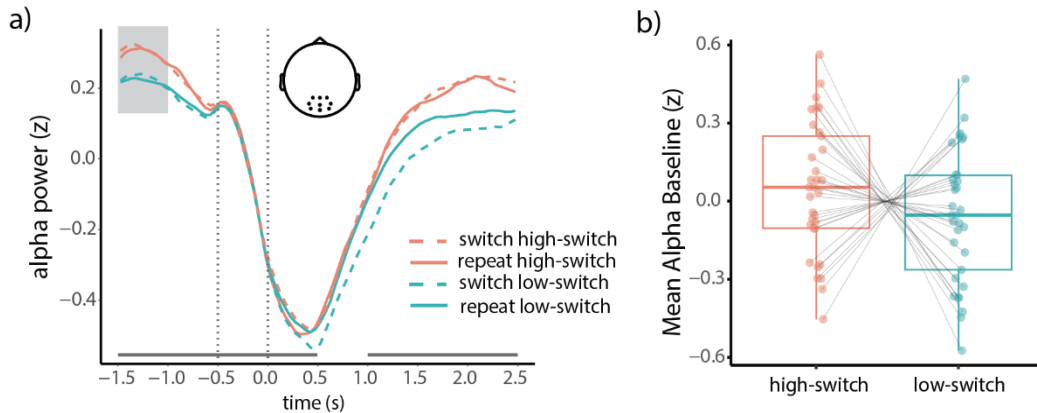


**Figure 8. Switch frequency modulates posterior alpha power.** a) Average posterior alpha power for each condition. The grey dotted lines indicate cue onset and stimulus onset. The horizontal bars indicate the time periods of significant differences between switch-frequency conditions. The grey box indicates the time window used for panel b and for the single-trial alpha values that formed the input for Equation 16. The scalp plot shows the posterior electrodes included in the analyses and figures. b) Average precue alpha power during the marked time period for each participant and switch frequency. The black line shows the average switch-frequency effect on alpha power. Note that at the level of individual participants the effect of switch frequency is confounded by session effects (e.g., a practice effect).

Our results suggest that adaptation of gain to switch frequency was tracked by both baseline pupil size and precue alpha power. To determine the extent to which these two physiological measures were related to one another, we residualized both for external factors (e.g., time on task, see *Equations 13, 15*) and then conducted a mixed model analysis. Trials with a larger baseline pupil size were associated with a larger precue alpha power (Figure 9; *Equation 16*, linear effect:  $\beta = 4.00$ , 95% CI [2.18, 5.82],  $t(8962) = 4.32$ ,  $p < .001$ ), at least in the lower range of pupil sizes. In the higher range, the relationship leveled off, resulting in a negative quadratic trend ( $\beta = -2.01$ , 95% CI [-3.80, -0.22],  $t(8962) = -2.19$ ,  $p = .03$ ). A significant interaction between this quadratic trend and switch-frequency ( $\beta = 3.67$ , 95% CI [1.15, 6.18],  $t(8962) = 2.86$ ,  $p = .004$ ) was driven by the largest pupil bin of the high-switch condition, which forced the overall trend in this condition to be more linear. Overall, these results indicate a complex relationship between trial-wise variation in baseline pupil size and precue alpha power, possibly reflecting a common mechanism when pupil sizes are small and different mechanisms when pupil sizes are large.

Lastly, we conducted a permutation cluster analysis across all electrodes and time points in the alpha band, as previous research has found a significant interaction between switch frequency and task transition in the post-cue interval (Siqi-Liu et al., 2022). That study identified a cluster of time points (0.1 to 0.5 s after cue onset) that showed stronger posterior alpha power on task-switch trials than on repeat trials, but only in the high-switch condition. We did not replicate this finding. We also did not find any other significant clusters in the period between the cue and the stimulus.

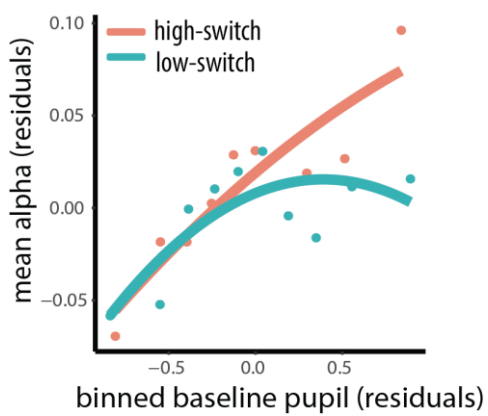


**Figure 9. Trial-by-trial relationship between precue posterior alpha power and baseline pupil size.** Precue posterior alpha power has significant linear and quadratic relationships with baseline pupil size in both switch-frequency conditions, with a stronger linear trend in the high-switch condition. To visualize this relationship, we divided the residuals of baseline pupil size into 10 bins with equal numbers of observations, separately for each participant and frequency condition, and then averaged across participants.

## 5. General Discussion

In this article we presented a mechanistic model that provided a formally rigorous, normative account of the trade-offs between both cognitive stability versus flexibility (Cools, 2019; Goschke, 2003) and response speed versus accuracy (Balci et al., 2011; Bogacz et al., 2006), in terms of RR optimization. Using a non-linear dynamical systems model of task switching (Jongkees et al., 2023), we replicated and extended previous computational work (Musslick et al., 2019, 2018) showing that a trade-off between flexible task switching and cross-task interference can be explained in terms of attractor dynamics associated with changes in control. Crucially, model simulations showed that this trade-off is not always clearly reflected in traditional measures of behavior – the task-switch cost and the response-incongruence cost. Instead, latent variables derived from model fits to data provided a more nuanced analysis of adaptive control.

Here we defined stability as the strength with which task representations were expressed in a processing system, and flexibility as the time required to transition between tasks. In our model, these attributes were regulated by the “intensity” of control signals, implemented as changes in gain over the control units responsible for biasing stimulus processing in the model. Higher intensity augments and narrows processing to task-relevant inputs but also leads to slower reconfiguration of control. Conversely, weaker control broadens processing to task-irrelevant inputs but allows for faster reconfiguration. These dynamics of control have been conceptualized as attractor basins in a potential energy landscape, with deep attractors conferring greater stability but also increasing the distance between attractors (Durstewitz & Seamans, 2008; Musslick & Cohen, 2021; Ueltzhöffer et al., 2015). Normative analyses showed that optimal overall task performance (in terms of maximizing RR) is achieved by adopting lower intensity of control – that is, a shallower attractor landscape – when task-switches are frequent. Participants in a behavioral experiment conformed to this model prediction,

demonstrating improved task-switching performance when switches were frequent at the cost of increased cross-task interference. These changes in control and behavior were accompanied by changes in pupil size, a physiological marker of neural gain (Aston-Jones & Cohen, 2005; Eldar et al., 2013; Gilzenrat et al., 2010; Tromp et al., 2022; Warren et al., 2016) as well as changes in posterior baseline alpha power.

Below, we discuss key implications of our findings for the broader literature, as well as avenues for future research.

### **The trade-off between stability and flexibility**

Model simulations indicated that the intensity of control signals has distinct, non-linear effects on performance in a classic 2AFC task-switching paradigm. Intensity of control signals was regulated by the gain of a sigmoidal activation function on task-representing control units. Higher gain leads to higher intensity of control and monotonically improves performance on task-repeat trials, by increasing activity in the task-relevant processing pathway and decreasing activity in the irrelevant pathway. Task-switch trials initially also improve with higher gain, provided that a preparation interval (i.e., the CSI) allows some time for reconfiguration of control before the onset of the target stimulus. However, beyond a certain point, increases in gain impair performance on task-switch trials, as task attractors become too distant to transition between during the CSI. This is especially detrimental to performance when stimuli are response-incongruent because, during the transition between attractors, processing of the previously-relevant, now task-irrelevant stimulus dimension activates the incorrect response.

These effects of higher gain produce monotonic increases in the task-switch cost, which is the performance difference between task-switch and repeat trials. The switch cost is traditionally taken as an inverse measure of *flexibility*, assumed to reflect the time needed to reconfigure control (Allport et al., 1994; Meiran, 1996; Monsell, 2003). In line with this interpretation, our

simulations showed that the switch cost rises as higher gain leads to increasingly distant attractors. However, the effects of gain were more complex for the response-incongruence cost, which is the performance difference between response-incongruent and congruent trials. The incongruence cost is traditionally interpreted as an inverse measure of *stability*, assumed to reflect interference or conflict between tasks and/or responses (Braem et al., 2019; Duthoo et al., 2014; Gratton et al., 1992). In line with traditional views, the incongruence cost on task-repeat trials decreases monotonically with higher gain, eventually reaching a plateau at which the uncued task reaches a minimal level of activation. Conversely, the incongruence cost on task-switch trials follows a non-monotonic, U-shaped pattern, initially decreasing but eventually increasing with higher gain. This is because with high gain on task-switch, response-incongruent trials, processing of the task-irrelevant dimension activates the incorrect response, which is exacerbated as the system takes longer to transition away from the attractor corresponding to the previously-cued task.

As discussed in previous sections, the U-shaped relationship between gain and incongruence costs on task-switch trials has major implications for the interpretation of this cost as a measure of stability. Because increases in gain can reduce the incongruence cost (in the lower range of gain) but also increase it (in the higher range of gain), it is possible for the mean incongruence cost across participants to not change even if all participants increase their stability (cf. (Musslick et al., 2019)). It is even possible for both switch and incongruence costs to increase, as both costs are driven by performance on task-switch response-incongruent trials. Consistent with this possibility, we observed such a joint increase in both costs in our analysis of RR optimization to task-switch frequency.

These findings are particularly relevant, considering empirical findings offered as evidence against an obligatory trade-off between stability and flexibility (Egner, 2023; Mayr & Grätz, 2024). Our findings suggest that the interpretation of such evidence warrants closer

examination, both with respect to definitions of stability versus flexibility in terms of mechanisms of control rather than behavioral measures, as well as potential interactions with the speed-accuracy trade-off through adjustments of decision threshold — effects that can be subtle and complex, and thus demand formally rigorous models to identify. Below we consider how this approach may address some of the findings used to challenge the idea of a stability-flexibility tradeoff.

*Positive correlation between switch and incongruence costs.* A recent series of studies aimed to orthogonally manipulate the contextual demand for stability and flexibility (Geddert & Egner, 2022, 2024; 2025). The assumptions and conclusions in these studies all had high face validity. First, they assumed that changes in switch and incongruence costs reflect changes in flexibility and stability, respectively. Second, they assumed that a trade-off between stability and flexibility does not allow the two costs to both increase or decrease at the same time. Third, they assumed, as we did, that the frequency of task-switches determines the demand for flexibility, with higher frequencies requiring greater flexibility. Fourth, and in line with the abundant literature on conflict adaptation (Braem et al., 2019; Duthoo et al., 2014; Gratton et al., 1992), they assumed that the frequency of response-incongruent stimuli determines the demand for stability, with higher frequencies requiring greater stability.

These experiments (Geddert & Egner, 2022, 2024; 2025) used a task-switching paradigm similar to the one we used, but with the important difference that the frequencies of task-switches and response-incongruent stimuli were manipulated independently to be either low (25%) or high (75%). This joint manipulation has not been used often in task-switching studies, which have typically manipulated the frequency of task-switches while fixing the frequency of response-incongruent stimuli at 50%, as we did. The key performance contrast was between the condition in which both frequencies were low (here denoted as 25/25) versus when both frequencies were high (denoted as 75/75). Based on the assumptions outlined above, the 75/75

condition should demand an increase in flexibility *and* stability, reflected in a simultaneous decrease in switch costs *and* incongruence costs. However, it was assumed that such an observation would violate a trade-off. Participants in the experiments exhibited such an effect – smaller switch costs and smaller incongruence costs in the 75/75 as compared to the 25/25 condition – that was interpreted as evidence against an obligatory trade-off between stability and flexibility.

Our findings suggest an alternative interpretation of these behavioral findings, that remains consistent with an underlying tension between stability and flexibility in terms of control. Specifically, our simulations demonstrate how changes in the switch and incongruence costs can correlate positively with one another, even though the attractor dynamics of control are subject to a trade-off between flexible reconfiguration and suppression of task-irrelevant processing. That is, a simultaneous increase in both costs can occur when incompatible task representations are expressed with a sufficiently large distance between them, which increases the time required to transition between tasks (the switch cost) and increases processing of task-irrelevant stimuli during that transition (the incongruence cost). Importantly, this shows that greater stability (i.e., high gain) does not necessarily benefit performance on response-incongruent trials in a task-switching paradigm. This contrasts with the majority of studies on conflict adaptation, which traditionally do not involve task switching (Braem et al., 2019; Duthoo et al., 2014; Gratton et al., 1992). Most importantly, the empirical finding above – of smaller switch costs *and* smaller incongruence costs in the 75/75 condition – is consistent with a normative prediction concerning the stability-flexibility trade-off as formalized in the present paper. By definition, the 25/25 condition consists of 75% task-repeat trials, that we showed benefit from high gain (Figure 3a). Furthermore, of the 25% task-switches, 18.75% are response-congruent, which are only mildly impaired by high gain: Even if that leads to stronger processing of the task-irrelevant stimulus, it still activates the correct response. Thus, only

6.25% of trials in the 25/25 condition (i.e., trials involving a task-switch *and* response-incongruent stimuli) are penalized for high gain, so that, on average, high gain maximizes RR. In contrast, in the 75/75 condition more than half of all trials (56.25%) are penalized by high gain, so that the gain that maximizes RR will be lower. As a result, the average switch cost and incongruence cost are predictably higher in the 25/25 condition, due to the detrimental effect of high gain on task-switch, response-incongruent trials. This alternative interpretation of results is consistent with the observation that: for task-repeat trials, performance is superior in the 25/25 as compared to 75/75 condition irrespective of congruence; whereas, for switch trials, performance is roughly comparable across frequency conditions for congruent trials but markedly worse on incongruent trials in the 25/25 vs 75/75 condition.

In summary, our findings suggest that a model in which control manipulates gain to maximize RR can account for the complex pattern of behavioral effects observed under joint manipulations of switch and incongruence frequency and, in particular, demonstrates that the positive correlation between switch and incongruence costs is consistent with an underlying trade-off between stability and flexibility of task representations.

*Observations from clinical populations.* These have also been used to argue for the independence of stability and flexibility (Egner, 2023). For example, it has been noted that individuals with attention-deficit hyperactivity disorder (ADHD) and schizophrenia can exhibit paradoxically co-occurring deficits in task focus (stability) and task switching (flexibility) (Egner, 2023). On the one hand, our model simulations indicate that levels of gain that are too low can compromise overall performance—that is, on both task-switch and repeat trials—by providing little contrast in activity between task-relevant and task-irrelevant processing pathways. Accordingly, reduced gain has been suggested to underlie various characteristics of ADHD (Hauser et al., 2016). Importantly, however, deficits in stability and flexibility do not appear to occur *at the same time*. Instead, ADHD is characterized by alternating periods of high

distractibility (flexibility) and periods of hyperfocus (stability) (Hupfeld et al., 2019; Groen et al., 2020). Thus, the key impairment appears to be in context-sensitive regulation of these two extremes, which is consistent with a tension between them.

*Distinct neural mechanisms.* One explanation for how independent stability and flexibility could be implemented in the brain has relied on neuroscientific evidence of distinct neural systems (Egner, 2023), with the prefrontal cortex (PFC) responsible for stability of task representations and the basal ganglia (BG) responsible for flexible gating of relevant inputs. However, the functionalities of these two systems are, at the least, widely believed to be closely intertwined (Alexander et al., 1986; Durstewitz & Seamans, 2008), and arguably reflect tightly interacting subcomponents of an integrated system. For example, according to an influential neuroscientific model, a transient increase in dopamine within BG triggers the gating of inputs to PFC that can implement a task-switch (O'Reilly & Frank, 2006). In PFC this is thought to toggle neural populations into an activity regime that corresponds to a shallow attractor landscape, making the system more receptive to incoming inputs. However, at the same time, this flexible gating process also makes the system more susceptible to noise and interference from competing and task-irrelevant processes. This presumably contributes to the trial-level interaction between task transition and congruence, in which incongruence costs tend to be larger on task-switch trials (Kiesel et al., 2010; Meiran, 2000; Rogers & Monsell, 1995). Converging behavioral evidence comes from the finding that repetition or alternation of entirely task-irrelevant stimulus features only affects performance during task-switches (Dreisbach & Haider, 2008), when the system is most susceptible to irrelevant information. Particularly noteworthy is the finding that distractor stimuli are more decodable in EEG during a task-switch (Hubbard et al., 2019), indicating elevated processing of distractors which is consistent with the BG momentarily driving the cognitive system into a regime of shallow attractors to implement a task-switch. In other words, even if flexible gating is a BG-driven process, its

effects cannot easily be separated from the mechanisms responsible for stable maintenance of task representations in PFC (i.e. gain modulation) and therefore do not clearly constitute evidence for the independence of stability and flexibility.

Another suggestion for how stability and flexibility may be correlated rather than in tension is in terms of “cognitive maps”, in which the allocation of control increases the resolution of task representations encoded in long-term memory (Mayr & Grätz, 2024). This would reduce interference from competing tasks (increasing stability) while also making tasks more “findable” on the map (increasing flexibility). However, it remains unclear whether reduced interference from competing tasks can be achieved, in practice, without compromising flexibility. For example, it is possible that the activity dynamics required to encode a task representation with higher resolution also lead to more “inertia” of this activity upon a task-switch (cf. Allport et al., 1994) and thereby lead to impaired performance when a different representation needs to be activated. There is indeed evidence that such inertia effects emerge for distinctive task representations, even in task-optimized recurrent neural networks that lack hand-crafted structural mechanisms (Ritz et al., 2024).

*Normative constraints.* Lastly, assuming it is possible for stability and flexibility to vary independently, it remains unclear from a resource-rational point of view why participants would not always maximize their stability and flexibility to achieve the highest possible RR. An explanation in terms of cognitive “effort” requires a precise definition of the term and a mechanistic implementation of how this constrains the allocation of stability and flexibility. In our own work, we align with the growing consensus that the experience of cognitive effort is a phenomenological counterpart to an opportunity cost in time (Kurzban et al., 2013; Shenhav et al., 2013, 2017), which provides a normative explanation for a constraint on the intensity of control (i.e., stability) as mediated through gain, because of the increased time necessary to

disengage from and switch between tasks (i.e., flexibility) (cf. Musslick et al., 2019, 2018; Musslick & Cohen, 2021).

To conclude, whether stability and flexibility are inextricably coupled remains an important and open question. Previous work (Musslick & Cohen, 2021; Usher & McClelland, 2001) together with that reported here strongly suggest that the non-linear, competitive, and recurrent dynamical mechanisms thought to occur in the brain make it difficult to fully isolate these two factors, at least under conditions in which the relevant tasks are incompatible with one another. This presents an interesting challenge for future work to develop mechanistic and neurally-plausible models in which stability and flexibility can be dissociated. Here, we simply point out that standard behavioral measures – RT, accuracy, and differences in these under various task conditions – may be insufficient *on their own* to adjudicate this issue. Rather, quantitatively, mechanistic models, coupled with efforts to measure latent variables introduced by such models, are needed to determine whether, in the case of human cognition, and its implementation in the brain – there is a fundamental trade-off between stability and flexibility. Our findings suggest that this remains a plausible possibility.

### **The trade-off between speed and accuracy**

In the course of considering the stability-flexibility trade-off, we also examined the extent to which this interacts with optimization of the speed-accuracy trade-off. This was motivated by well-established findings that participants jointly optimize response speed and accuracy to maximize the average RR (Bogacz et al., 2006; Gold & Shadlen, 2002). This has been formalized using a highly influential model of decision making (Ratcliff, 1978), in which the trade-off between speed and accuracy is governed by the height of a threshold during noisy evidence accumulation over time. The optimal threshold can be formalized as the one that maximizes average RR. Given that task switching is associated with slower, less accurate

performance, it is plausible that the optimal speed-accuracy trade-off also depends on the frequency of task-switches. To comprehensively test this hypothesis, we took into account that participants might not always achieve optimal RR due to joint optimization of RR and accuracy (Balci et al., 2011; Bogacz et al., 2006, 2010), and that the speed-accuracy trade-off might be adjusted over the course of evidence accumulation—that is, thresholds that “collapse” during a trial (Boehm et al., 2020; Cisek et al., 2009).

Our analyses of RR optimization indicated that the effect of switch frequency on the optimal speed-accuracy trade-off is in fact limited. The optimal starting point of a collapsing threshold only diverges for different frequencies when sensitivity to errors is high – that is, when there is a strong emphasis on accuracy. An increase in the optimal starting point of a collapsing threshold is associated with an increase in its collapse rate, indicating that higher response caution at the start of a trial is accompanied by a stronger decrease in caution over time. This is likely driven by the response deadline, because higher thresholds make it increasingly likely that the deadline is missed unless a compensatory mechanism, a progressive collapse of the threshold, avoids very slow responses. Our simulations indicate that such a strategy can lead to small improvements in RR, although the benefits might not be sufficient to incentivize adaptation to switch frequency, especially in the presence of any variability in response processing (e.g., decision and/or execution noise).

Model fits to the empirical data suggested that participants did not adjust their threshold and collapse rate to switch frequency. However, it did appear that they did so in other ways, consistent with RR optimization of the speed-accuracy trade-off. Notably, the height of participants’ initial threshold was relatively high overall, indicating that participants emphasized both accuracy and RR. However, consistent with prior work on practice effects (Balci et al., 2011) participants adopted lower, more RR-optimal thresholds in the second session of the experiment. Moreover, we observed that models with a collapsing threshold

provided a superior fit to the data as compared to a model with static thresholds, by better capturing the right tail of the RT distribution – that is, the responses that were close to the deadline. This indicates that participants did adjust their speed-accuracy trade-off over the course of a trial, and notably did so to a roughly optimal extent.

Regardless of whether participants adjusted their speed-accuracy trade-off to task-switch frequency, our simulation results underscore the importance of considering individual differences in decision threshold, as these can strongly influence the switch and incongruence cost. This further complicates the interpretation of these measures in terms of stability and flexibility. Because differences in threshold produce similar increases or decreases in the two costs, care must be taken to control for this effect when comparing the costs across participants or task conditions.

### **Neurophysiological correlates of adaptive control**

The computational and behavioral adjustments we observed in our behavioral experiment were accompanied by patterns of neurophysiological data that provide further insight into the mechanisms underlying task switching. Because participants did not adjust their speed-accuracy trade-off to task-switch frequency, we focus here on interpreting observations related to changes in the frequency of task switching, and what these may reveal about stability versus flexibility of processing.

*Pupilometric findings.* Our findings regarding pupil size align with a growing body of data suggesting that catecholaminergic systems – and the LC in particular – play an important role in governing the stability-flexibility trade-off (Aston-Jones & Cohen, 2005; Bouret & Sara, 2005; Janitzky et al., 2015; McBurney-Lin et al., 2022; Sales et al., 2019; Shine, 2023).

First, we found that the high-switch condition, which requires increased cognitive flexibility, was associated with larger baseline pupil size. This finding is consistent with previous work that has found a link between increased baseline pupil size and behavioral measures of task disengagement and exploration, two other behavioral signatures of cognitive flexibility (Devauges & Sara, 1990; Gilzenrat et al., 2010; Hayes & Petrov, 2016; Jepma & Nieuwenhuis, 2011; Lapiz et al., 2007; Pajkossy et al., 2018; Seu et al., 2009; Shourkeshti et al., 2023). Recent research in mice has provided further support linking this to the noradrenergic system: Optogenetically boosting LC activity increases pupil size and enhances behavioral flexibility (McBurney-Lin et al., 2022). Furthermore, drugs that increase tonic NE levels (i.e., mimic the effects of elevated NE release that characterize the tonic LC mode) have been found to facilitate reversal learning and attentional-set shifting monkeys and rats (Devauges & Sara, 1990; Lapiz et al., 2007; Seu et al., 2009). Together with prior computational modeling results (e.g., McClure et al., 2005), these findings suggest that increasing tonic LC activity is a general mechanism for shifting to a more flexible brain state, regardless of whether the need for cognitive flexibility is signaled by implicit or explicit cues.

We found that the high-switch condition was also associated with higher maximum pupil dilation. This is consistent with prominent theories that suggest phasic bursts of LC activity enable rapid network reorganization in support of immediate cognitive demands. The possibility that these phasic bursts were enhanced in the high-switch condition is in line with the idea that in more volatile contexts it is rational to respond to change with a stronger network reorganization. In line with the network reorganization hypothesis, work in primates shows that activation of the LC promotes the transition from one stable state to another in the anterior cingulate cortex (Joshi & Gold, 2022), a brain area that is heavily involved in cognitive control (Botvinick et al., 1999; Holroyd & McClure, 2015; Shenhav et al., 2013). In terms of dynamical systems, it has been proposed that norepinephrine bursts briefly flatten the potential energy

landscape to facilitate brain-state transitions (Munn et al., 2021; Nassar, 2024). When viewed through this lens, our pupil findings suggest that the high-switch condition was characterized by a tonically flattened energy landscape (promoting sustained cognitive flexibility) as well as stronger cue-evoked landscape resets (facilitating rapid brain-state transitions on task-switch trials).

*EEG findings.* Our EEG measurements showed that baseline alpha power (measured during the intertrial interval) was higher in the high-switch frequency condition. Suppression of alpha power is seen as a signature of high task engagement and cognitive effort (Macdonald et al., 2011). This is beneficial when the task set used in the previous trial should be maintained, but detrimental when switching to another task set is required. Our finding, and that of others (Liu & Yeung, 2020) of increased baseline alpha power in high-switch frequency condition thus supports the hypothesis that adaptation to a high-switch condition is facilitated through a sustained decrease in control intensity.

Our finding that baseline pupil size and baseline alpha power were both sensitive to switch frequency led us to examine the trial-by-trial relationship between these physiological measures. Alpha power increased linearly with baseline pupil size in the lower range of pupil size, but then leveled off for larger pupil sizes, resulting in statistically significant linear and quadratic relationships. A similarly shaped relationship between the two measures has been reported previously (Podvalny et al., 2021; van Kempen et al., 2019), suggesting that they are governed by distinct but related mechanisms. However, other relationships between pupil size and alpha power have also been reported, including strictly linear, U-shaped, and no relationships (Ceh et al., 2020; Hong et al., 2014; Pfeffer et al., 2022; Pilipenko & Samaha, 2024; Waschke et al., 2019). This indicates that the relationship between these two measures is complex, and perhaps task dependent. More research is needed to understand the unique and

common influences of pre-trial pupil-linked arousal and oscillatory alpha power on cognitive flexibility.

### **Open questions and future research**

The present work raises several questions that remain to be addressed. Some of these have already been noted above, including the extent to which stability and flexibility are in tension with one another and their interaction with the speed-accuracy trade-off. Here, we turn to a few additional questions that we believe are important to address in future research.

Our work focused on how adaptation of control optimizes performance in a context-sensitive manner. However, our model does not address the mechanisms through which a (changing) need for control is detected or learned. In this sense, the control units in our model reflect the *execution* of control but not the *decision* of whether and how intensely to exert it. To fully capture the dynamics and mechanisms of adaptive control, future models need to incorporate mechanisms responsible for monitoring and evaluating the relative benefits of different modes of processing in relation to changing environmental demands. Such modeling work could build on the now well-established roles for the BG in reinforcement learning of control (Braver & Cohen, 2000; Frank et al., 2001) and anterior cingulate cortex in performance monitoring and weighing the costs of control (Botvinick et al., 2004; Shenhav et al., 2013), theories of adaptive gain and how this optimizes performance on different timescales (Aston-Jones & Cohen, 2005), and growing evidence that medial frontal areas track statistics of the environment such as volatility and opportunity cost while also being well positioned to modulate signaling from brainstem neuromodulatory mechanisms based on these statistics (Cools, 2019).

While our study highlights the role of norepinephrine in modulating the stability-flexibility trade-off, it is crucial to acknowledge the significant evidence supporting dopamine's involvement in this trade-off as well. Dopamine has been extensively studied for its role in the

stability-flexibility trade-off, particularly through its actions on distinct receptor pathways in the PFC. According to the dual-state theory of PFC dopamine function, D1 receptor activation is associated with increased cognitive stability, enhancing the maintenance of goal-relevant information, whereas D2 receptor activation facilitates cognitive flexibility, allowing for rapid switching between different mental representations (Durstewitz & Seamans, 2008). Furthermore, a recent review by Cools (2019) summarizes compelling evidence that dopamine's influence extends beyond the PFC to other brain regions involved in the stability-flexibility trade-off. Specifically, the review highlights that dopaminergic activity in the striatum is crucial for shifting between tasks or strategies, which relates to the BG-driven gating system discussed above. This suggests that dopamine not only supports the maintenance of stable cognitive states but also enables the exploration of alternative strategies when necessary. Systematic comparisons between these dopaminergic mechanisms, the noradrenergic influences revealed by animal studies and suggested by our pupil findings, and their potential interactions (e.g., McClure et al., 2005) will be crucial for a more comprehensive understanding of the neurochemical bases underlying the stability-flexibility trade-off.

Another avenue for future research is to consider the tonic (across-trial) versus phasic (within-trial) nature of changes in control. In the present work, a modulation of the depth of attractors occurred in a condition-dependent manner, by constraining the gain on control units to vary between switch frequency conditions but to be fixed within and across trials in each condition. On the one hand, this broadly aligns with ideas about tonic adjustment of control over relatively long timescales (Aston-Jones & Cohen, 2005) and is consistent with our pre-trial (i.e., not event-related) physiological measures of pupil size and posterior baseline alpha power. On the other hand, as discussed above, both dopamine and norepinephrine are believed to also implement rapid, phasic changes in control, by changing the gain of prefrontal neurons over a trial-by-trial or even within-trial timeframe that is driven by burst activity in the midbrain. Such

phasic changes in control are consistent with the larger stimulus-evoked pupil dilations that we observed when task-switch frequency was high, even when we controlled for pre-trial pupil size and RT, which are factors known to influence pupil dilations (Gilzenrat et al., 2010; Murphy et al., 2016). Various models in the literature implement rapid changes in control through phasic gain modulation or otherwise multiplicative effects, both in terms of input and output gating, to capture the effects of dopaminergic and noradrenergic systems (Aston-Jones & Cohen, 2005; Flesch et al., 2022; O'Reilly & Frank, 2006; Ritz & Shenhav, 2024; Sara & Bouret, 2012; Yu & Dayan, 2005). How our model relates to these gating models remains an important direction for future research.

Lastly, our work was restricted to performance on 2AFC tasks. This is in line with the predominant focus on such tasks in the decision making literature, and thus benefits from the extensive modeling work in this area. However, in the real world people are confronted with a near-infinite number of possible tasks and choices. Although some work has investigated multi-alternative decision making, corresponding models are often not well-behaved, experiencing issues with parameter recovery and non-identifiability of different models (Callaway et al., 2021; McMillen & Holmes, 2006; Miletic et al., 2017). Nevertheless, progress in this domain is needed for a comprehensive understanding of decision making and control. For example, it would help clarify whether the adaptation of control signal intensity as described in the present work is of a more general or task-specific nature. This is relevant, considering evidence that the effects of task-switch frequency on switch costs can be task-specific (Siqi-Liu & Egner, 2023), which is in line with the proposal that prefrontal gain can be adjusted not only in a global but also local manner (Mather et al., 2016).

## Conclusion

We have provided a mechanistically explicit, normative account of performance in task switching paradigms that addresses the trade-off between cognitive stability and flexibility and how this interacts with the trade-off between response speed and accuracy. We demonstrated that traditional measures of behavior – the task-switch and response-incongruence costs – can be poor indicators of their assumed latent variables. For this reason, it is important that studies include formally rigorous, mechanistic process models that can make quantitative predictions, capture individual differences, and account for the complex interactions that can occur among multiple, often subtle factors that influence decision-making processes and their outcome in performance.

## Acknowledgements

This work was supported by funding from the Vici grant awarded to Sander Nieuwenhuis and the Veni grant awarded to Bryant Jongkees, both financed by the Dutch Research Council (NWO), with project numbers VI.C.181.032 and VI.Veni.221G.084, respectively.

## Transparency and openness

We reported how we determined our sample size, all data exclusions (if any), all manipulations, and all measures in the study. All data, analysis code, and research materials are available at <https://osf.io/k4cjf/>. This study's design and its analyses were not pre-registered.

## Author contributions (CRediT)

Jeshua Tromp: conceptualization, data curation, formal analysis, visualization, writing—original draft

Sander Nieuwenhuis: conceptualization, funding acquisition, project administration, supervision, writing—review and editing

Jonathan Cohen: conceptualization, software, writing—review and editing

Bryant Jongkees: conceptualization, data curation, formal analysis, funding acquisition, methodology, project administration, supervision, visualization, writing—original draft, writing—review and editing

## Supplementary Materials

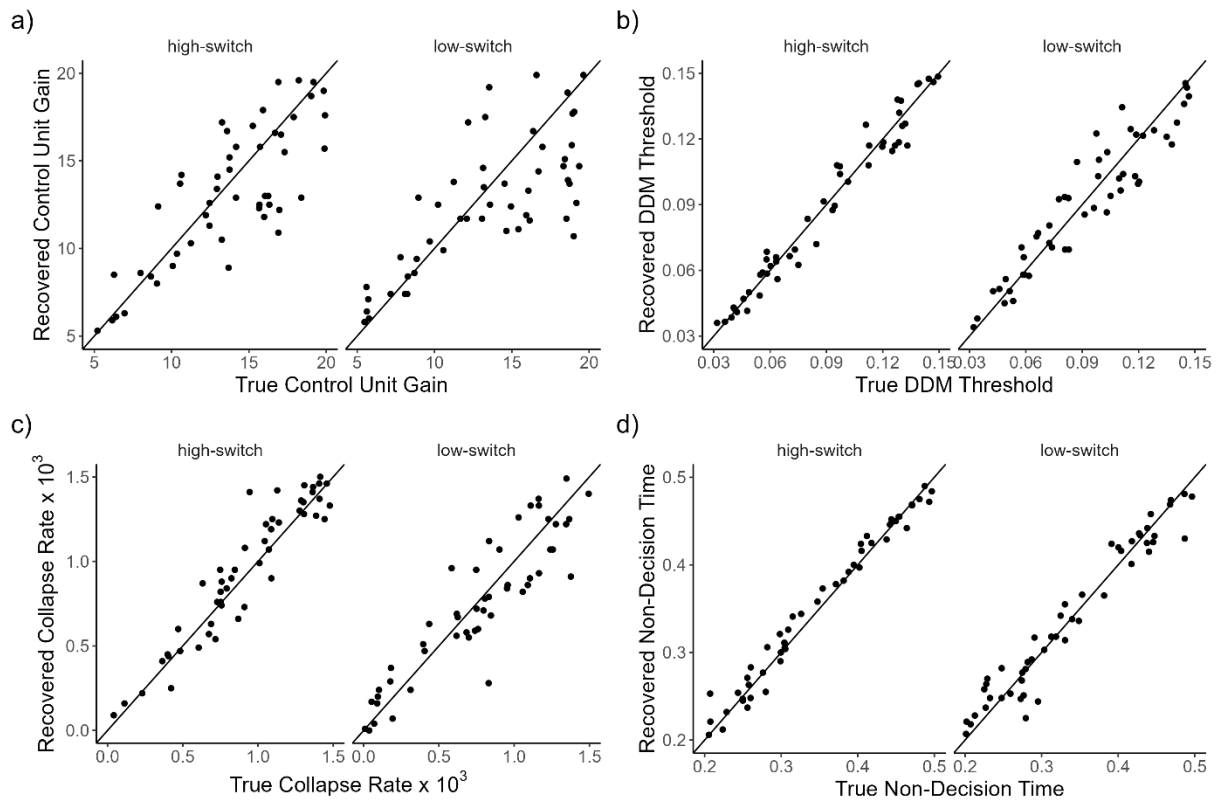


**Figure S1. Parameter recovery.** True and recovered model parameters for a) gain on the control units, b) starting point of the decision threshold, c) collapse rate of the decision threshold, and d) non-decision time (in seconds). The diagonal line represents perfect recovery.

To assess recoverability of model parameters, we simulated 50 trial sequences of 544 trials each, where 272 trials included a 25% switch frequency (“low-switch”) and 272 trials included a 75% switch frequency (“high-switch”). The frequency of response-incongruent trials was 50% and counterbalanced across task-switch and repeat trials in each frequency condition. For each trial sequence and switch frequency, random parameter values were sampled from a uniform distribution (gain of control units: 5 to 20, starting point of the decision threshold, 0.03 to 0.15, collapse rate of the threshold, 0 to 0.0015, non-decision time: 0.2 to 0.5). We restricted the parameter ranges to those observed in empirical data, to ensure we selected plausible parameter values. We subsequently fit the model to simulated data with the same procedure as

described in the main text (5000 iterations of the CMA-ES sampler). Recovery of decision threshold, collapse rate, and non-decision time was excellent for all conditions (Pearson correlation coefficients ranging from 0.90 to 0.99), while recovery of gain was lower but still good (Pearson correlation coefficient of 0.75 in the low-switch condition, 0.80 in the high-switch condition). Recovery of high gain values becomes harder in the low-switch condition, presumably because higher values of gain (i.e., a steepening of the sigmoid function, Eq. 3) increasingly lead to asymptotic task performance except on task-switch, response-incongruent trials, which are least frequent in the low-switch condition. Importantly, recovery of gain is not biased towards lower or higher values, nor does it trade off against other model parameters as indicated by uncorrelated residuals ( $p_s > .586$ ). The residuals of threshold, collapse rate, and non-decision time do trade off against each other ( $p_s < 0.001$ ), but this poses no major issue considering the high recovery rate.

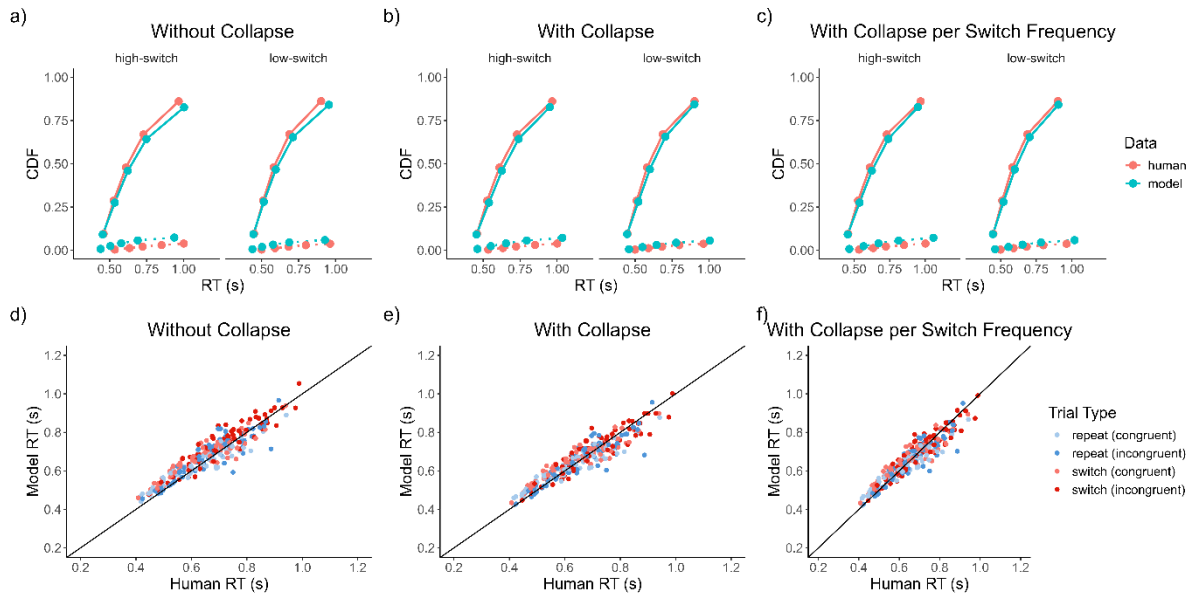


**Figure S2. Posterior predictive check.** (a-c) Cumulative distribution functions of RT in human and model data, averaged across participants and plotted as a function of task-switch frequency, correct trials (solid lines), error trials (dashed lines), and models without a collapsing threshold, with a single collapse rate, and separate collapse rate per switch frequency. (d-f) Model fitted parameter estimates were used to simulate performance on the same trial sequences performed by participants. Each data point represents the mean performance of a participant, as a function of switch frequency, task transition, and congruence. The diagonal line represents perfect correspondence between human and model data.

To assess model fit to human data, we simulated performance using the participants' model-fitted parameter values and the same trial sequences they completed in the behavioral experiment. To average out stochasticity in the simulation process, each trial sequence was simulated 100 times. The cumulative distribution function (CDF) of RTs shows the model was able to capture the overall shape of the RT distribution (Figure S2a-c) and individual differences in human and model RT were highly correlated (Figure S2d-f, Pearson correlation coefficients of 0.928 and above). However, the models with a collapsing threshold were best able to capture the slowest responses, whereas the model with a static threshold produced RTs that were too

slow at the right tail of the distribution. The model with a single collapse rate for both switch frequencies provided the best fit for most participants, as indicated by lowest BIC scores: 23 out of 35 participants favored the model with a single collapse rate, 3 participants favored the model with separate collapse rates, and 9 participants favored the model without collapsing threshold.

### Tables with all statistics for mixed model analyses

The labels in parentheses indicate the contrast, coded as 0 and 1.

#### Equation 9

Effect	Estimate	Std. Error	df	t value	p-value
Intercept	0.0595	0.0716	34.24	0.831	0.412
Switch frequency (low vs. high)	0.0024	0.0096	14844	0.253	0.800
Task transition (switch vs. repeat)	-0.0809	0.0085	14844	-9.504	< .001
Congruence (incongruent vs. congruent)	0.1852	0.0198	14844	9.370	< .001
Digit condition 1	-0.0498	0.0297	14844	-1.677	0.094
Digit condition 2	-0.0171	0.0254	14844	-0.672	0.502
Digit condition 3	-0.1220	0.0298	14844	-4.089	< .001
Digit condition 4	0.1011	0.0255	14844	3.973	< .001
Digit condition 5	-0.1216	0.0300	14844	-4.058	< .001
Digit condition 6	0.1300	0.0256	14844	5.086	< .001
Previous transition (switch vs. repeat)	-0.0328	0.0085	14844	-3.856	< .001
Task transition × Previous transition	-0.0432	0.0085	14844	-5.071	< .001
Switch frequency × Task transition	0.0512	0.0096	14844	5.333	< .001
Switch frequency × Congruence	0.0161	0.0085	14844	1.898	0.058
Task transition × Congruence	-0.0188	0.0085	14844	-2.210	0.027

#### Equation 10

Effect	Estimate	Std. Error	z value	p-value
Intercept	-2.786	0.121	-23.10	< .001
Switch frequency (low vs. high)	0.026	0.038	0.686	0.493
Task transition (switch vs. repeat)	-0.163	0.034	-4.733	< .001
Congruence (incongruent vs. congruent)	-0.424	0.031	-13.57	< .001
Digit (continuous or coded ordinal)	0.021	0.011	1.963	0.0496
Previous transition (switch vs. repeat)	-0.107	0.033	-3.239	0.0012
Task transition × Previous trial	-0.084	0.033	-2.533	0.0113
Switch frequency × Task transition	0.042	0.037	1.131	0.258
Switch frequency × Congruence	0.075	0.034	2.182	0.0291
Task transition × Congruence	0.064	0.034	1.881	0.0599

**Equation 11**

<b>Effect</b>	<b>Estimate</b>	<b>Std. Error</b>	<b>df</b>	<b>t value</b>	<b>df</b>	<b>p-value</b>
<i>Gain</i>						
Switch frequency (low vs high)	-0.30	0.11	33	-2.70	33	0.010
Session number (first vs second)	-0.10	0.11	33	-0.87	33	0.390
Switch frequency × Session number	-0.18	0.12	33	-1.52	33	0.138
<i>Threshold</i>						
Switch frequency (low vs high)	0.08	0.08	33	1.07	33	0.294
Session number (first vs second)	0.34	0.08	33	4.31	33	< 0.001
Switch frequency × Session number	0.13	0.14	33	0.93	33	0.361
<i>Non-decision time</i>						
Switch frequency (low vs high)	-0.09	0.09	33	-1.09	33	0.286
Session number (first vs second)	0.00	0.09	33	0.00	33	0.997
Switch frequency × Session number	0.04	0.15	33	0.30	33	0.767

**Equation 13** (when used for obtaining residuals)

<b>Effect</b>	<b>Estimate</b>	<b>Std. Error</b>	<b>df</b>	<b>t value</b>	<b>p-value</b>
Intercept	-0.00007	0.1507	25.00	0.000	0.9997
Switch frequency (low vs high)	0.0171	0.0060	10664	2.829	0.0047*
Session number (first vs second)	-0.0794	0.0060	10664	13.150	<0.001
Peak pupil size on previous trial	0.1041	0.0062	10664	16.703	<0.001
Block	0.0727	0.0331	10664	2.199	0.0279
Block <sup>2</sup>	-0.0746	0.0331	10664	-2.257	0.0240
Blocktrial	-0.4234	0.0294	10664	-14.421	<0.001
Blocktrial <sup>2</sup>	0.2856	0.0290	10664	9.834	<0.001

\*In line with previous research (Rondeel et al., 2015; da Silva Castanheira et al., 2021), switch trials were characterized by larger cue-evoked pupil dilation.

**Equation 14**

<b>Effect</b>	<b>Estimate</b>	<b>Std. Error</b>	<b>df</b>	<b>t value</b>	<b>p-value</b>
Intercept	0.5303	0.0700	88.54	7.579	<0.001
Switch frequency (low vs. high)	0.0285	0.0096	11430	2.985	0.0029
Session number	-0.0334	0.0167	11440	-2.001	0.0454
Correct response	-0.5059	0.0421	11440	-12.008	<0.001
Response time (RT)	0.0384	0.0088	11450	4.393	<0.001
Baseline Pupil	-0.2355	0.0086	11430	-27.375	<0.001
Task-transition (switch vs. repeat)	-0.0275	0.0094	11430	-2.918	0.0035
Congruence (incongruent vs. congruent)	-0.0229	0.0082	11430	-2.783	0.0054
Cue shown x type 1	-0.2549	0.0141	11430	-18.052	<0.001
Cue shown x type 2	-0.3905	0.0142	11430	-27.583	<0.001
Cue shown x type 3	0.3356	0.0142	11430	23.697	<0.001
Block	0.0449	0.0450	11430	0.998	0.3183

Block <sup>2</sup>	-0.0554	0.0450	11430	-1.232	0.2181
Blocktrial	0.0029	0.0393	11430	0.073	0.9415
Blocktrial <sup>2</sup>	-0.0818	0.0390	11430	-2.096	0.0361

**Equation 15** (when used for obtaining residuals)

Effect	Estimate	Std. Error	df	t value	p-value
Intercept	0.0017	0.1383	32.00	0.013	0.9901
Switch frequency (low vs. high)	0.0272	0.0054	14170	5.049	<0.001
Session number	-0.0488	0.0054	14170	-9.049	<0.001
Block	0.0581	0.0295	14170	1.971	0.0487
Block <sup>2</sup>	-0.0212	0.0295	14170	-0.720	0.4716
Blocktrial	0.0600	0.0299	14170	2.006	0.0449
Blocktrial <sup>2</sup>	-0.0305	0.0285	14170	-1.068	0.2856

**Equation 16**

Effect	Estimate	Std. Error	df	t value	p-value
Intercept	0.0129	0.0095	8962	1.362	0.1734
BaselinePupil	3.9982	0.9256	8962	4.320	<0.001
BaselinePupil <sup>2</sup>	-2.0068	0.9172	8962	-2.188	0.0287
Switch frequency (low vs. high)	-0.0183	0.0133	8962	-1.369	0.1712
BaselinePupil x switch frequency	-1.3611	1.2819	8962	-1.062	0.2884
BaselinePupil <sup>2</sup> x switch frequency	3.6662	1.2810	8962	2.862	0.0042

## Bibliography

- Alexander, G. E., DeLong, M. R., & Strick, P. L. (1986). Parallel organization of functionally segregated circuits linking basal ganglia and cortex. *Annual Review of Neuroscience*, 9(1), 357–381.
- Allport, D. A., Styles, E. A., & Hsieh, S. (1994). Shifting intentional set: Exploring the dynamic control of tasks. *Attention and Performance 15: Conscious and Nonconscious Information Processing*, 15(945), 421–452.
- Aston-Jones, G., & Cohen, J. D. (2005). An integrative theory of locus coeruleus-norepinephrine function: adaptive gain and optimal performance. *Annual Review of Neuroscience*, 28, 403–450.
- Balci, F., Simen, P., Niyogi, R., Saxe, A., Hughes, J. A., Holmes, P., & Cohen, J. D. (2011). Acquisition of decision making criteria: reward rate ultimately beats accuracy. *Attention, Perception & Psychophysics*, 73(2), 640–657.
- Barkley, R. A. (1997). Behavioral inhibition, sustained attention, and executive functions: constructing a unifying theory of ADHD. *Psychological Bulletin*, 121(1), 65–94.
- Bates, D., Mächler, M., Bolker, B., & Walker, S. (2015). Fitting Linear Mixed-Effects Models Using lme4. *Journal of Statistical Software, Articles*, 67(1), 1–48.
- Boehm, U., van Maanen, L., Evans, N. J., Brown, S. D., & Wagenmakers, E.-J. (2020). A theoretical analysis of the reward rate optimality of collapsing decision criteria. *Attention, Perception & Psychophysics*, 82(3), 1520–1534.
- Bogacz, R., Brown, E., Moehlis, J., Holmes, P., & Cohen, J. D. (2006). The physics of optimal decision making: a formal analysis of models of performance in two-alternative forced-choice tasks. *Psychological Review*, 113(4), 700–765.

- Bogacz, R., Hu, P. T., Holmes, P. J., & Cohen, J. D. (2010). Do humans produce the speed-accuracy trade-off that maximizes reward rate? *Quarterly Journal of Experimental Psychology* (2006), 63(5), 863–891.
- Botvinick, Cohen, J. D., & Carter, C. S. (2004). Conflict monitoring and anterior cingulate cortex: an update. *Trends in Cognitive Sciences*, 8(12), 539–546.
- Botvinick, Nystrom, L. E., Fissell, K., Carter, C. S., & Cohen, J. D. (1999). Conflict monitoring versus selection-for-action in anterior cingulate cortex. *Nature*, 402(6758), 179–181.
- Bouret, S., & Sara, S. J. (2005). Network reset: a simplified overarching theory of locus coeruleus noradrenaline function. *Trends in Neurosciences*, 28(11), 574–582.
- Braem, S., Bugg, J. M., Schmidt, J. R., Crump, M. J. C., Weissman, D. H., Notebaert, W., & Egner, T. (2019). Measuring adaptive control in conflict tasks. *Trends in Cognitive Sciences*, 23(9), 769–783.
- Braver, T. S., & Cohen, J. D. (2000). On the control of control: The role of dopamine in regulating prefrontal function and working memory. *Attention and Performance*, 18, 712–737.
- Breton-Provencher, V., & Sur, M. (2019). Active control of arousal by a locus coeruleus GABAergic circuit. *Nature Neuroscience*, 22(2), 218–228.
- Brown, J. W., Reynolds, J. R., & Braver, T. S. (2007). A computational model of fractionated conflict-control mechanisms in task-switching. *Cognitive Psychology*, 55(1), 37–85.
- Callaway, F., Rangel, A., & Griffiths, T. L. (2021). Fixation patterns in simple choice reflect optimal information sampling. *PLoS Computational Biology*, 17(3), e1008863.
- Ceh, S. M., Annerer-Walcher, S., Körner, C., Rominger, C., Kober, S. E., Fink, A., & Benedek, M. (2020). Neurophysiological indicators of internal attention: An electroencephalography-eye-tracking coregistration study. *Brain and Behavior*, 10(10), e01790.

- Cisek, P., Puskas, G. A., & El-Murr, S. (2009). Decisions in changing conditions: the urgency-gating model. *The Journal of Neuroscience: The Official Journal of the Society for Neuroscience*, 29(37), 11560–11571.
- Cohen, J. D., Dunbar, K., & McClelland, J. (1990). On the control of automatic processes: A parallel distributed processing account of the Stroop effect. *Psychological Review*, 97(3), 332–361.
- Compton, R. J., Arnstein, D., Freedman, G., Dainer-Best, J., & Liss, A. (2011). Cognitive control in the intertrial interval: evidence from EEG alpha power: Cognitive control in the intertrial interval. *Psychophysiology*, 48(5), 583–590.
- Cools, R. (2019). Chemistry of the adaptive mind: Lessons from dopamine. *Neuron*, 104(1), 113–131.
- de Gee, J. W., Colizoli, O., Kloosterman, N. A., Knapen, T., Nieuwenhuis, S., & Donner, T. H. (2017). Dynamic modulation of decision biases by brainstem arousal systems. *eLife*, 6. <https://doi.org/10.7554/eLife.23232>
- Devauges, V., & Sara, S. J. (1990). Activation of the noradrenergic system facilitates an attentional shift in the rat. *Behavioural Brain Research*, 39(1), 19–28.
- Ditterich, J. (2006). Evidence for time-variant decision making. *The European Journal of Neuroscience*, 24(12), 3628–3641.
- Dreisbach, G., & Fröber, K. (2019). On how to be flexible (or not): Modulation of the stability-flexibility balance. *Current Directions in Psychological Science*, 28(1), 3–9.
- Dreisbach, G., & Haider, H. (2006). Preparatory adjustment of cognitive control in the task switching paradigm. *Psychonomic Bulletin & Review*, 13(2), 334–338.
- Dreisbach, G., & Haider, H. (2008). That's what task sets are for: shielding against irrelevant information. *Psychological Research*, 72(4), 355–361.

- Drugowitsch, J., Moreno-Bote, R., Churchland, A. K., Shadlen, M. N., & Pouget, A. (2012). The cost of accumulating evidence in perceptual decision making. *The Journal of Neuroscience: The Official Journal of the Society for Neuroscience*, 32(11), 3612–3628.
- Durstewitz, D., & Seamans, J. K. (2008). The dual-state theory of prefrontal cortex dopamine function with relevance to catechol-o-methyltransferase genotypes and schizophrenia. *Biological Psychiatry*, 64(9), 739–749.
- Duthoo, W., Abrahamse, E. L., Braem, S., Boehler, C. N., & Notebaert, W. (2014). The heterogeneous world of congruency sequence effects: an update. *Frontiers in Psychology*, 5, 1001.
- Egner. (2017). *The Wiley Handbook of Cognitive Control*.  
<https://doi.org/10.1002/9781118920497>
- Egner. (2023). Principles of cognitive control over task focus and task switching. *Nature Reviews Psychology*, 2(11), 702–714.
- Egner, Tobias, & Siqi-Liu, A. (2024). Insights into control over cognitive flexibility from studies of task-switching. *Current Opinion in Behavioral Sciences*, 55, 101342.
- Eldar, E., Cohen, J. D., & Niv, Y. (2013). The effects of neural gain on attention and learning. *Nature Neuroscience*, 16(8), 1146–1153.
- Ferguson, K. A., & Cardin, J. A. (2020). Mechanisms underlying gain modulation in the cortex. *Nature Reviews. Neuroscience*, 21(2), 80–92.
- Flesch, T., Juechems, K., Dumbalska, T., Saxe, A., & Summerfield, C. (2022). Orthogonal representations for robust context-dependent task performance in brains and neural networks. *Neuron*, 110(7), 1258-1270.e11.
- Frank, M. J., Loughry, B., & O'Reilly, R. C. (2001). Interactions between frontal cortex and basal ganglia in working memory: a computational model. *Cognitive, Affective & Behavioral Neuroscience*, 1(2), 137–160.

- Frazier, P., & Yu, A. J. (2007). Sequential hypothesis testing under stochastic deadlines. *Neural Information Processing Systems*, 20, 465–472.
- Geddert, R., & Egner, T. (2022). No need to choose: Independent regulation of cognitive stability and flexibility challenges the stability-flexibility trade-off. *Journal of Experimental Psychology. General*, 151(12), 3009–3027.
- Geddert, R., & Egner, T. (2024). Contextual control demands determine whether stability and flexibility trade off against each other. *Attention, Perception & Psychophysics*, 86(7), 2529–2551.
- Geddert, R., Madlon-Kay, S., O'Neill, K., Pearson, J., Egner, T. (2025). Modeling of control over task switching and cross-task interference supports a two-dimensional model of cognitive. *Psychonomic Bulletin & Review*.
- Gilzenrat, M. S., Nieuwenhuis, S., Jepma, M., & Cohen, J. D. (2010). Pupil diameter tracks changes in control state predicted by the adaptive gain theory of locus coeruleus function. *Cognitive, Affective & Behavioral Neuroscience*, 10(2), 252–269.
- Gladwin, T. E., & de Jong, R. (2005). Bursts of occipital theta and alpha amplitude preceding alternation and repetition trials in a task-switching experiment. *Biological Psychology*, 68(3), 309–329.
- Gold, J. I., & Shadlen, M. N. (2002). Banburismus and the brain. *Neuron*, 36(2), 299–308.
- Goschke. (2003). Voluntary action and cognitive control from a cognitive neuroscience perspective. *Voluntary Action: Brains, Minds, and Sociality.*, 379, 49–85.
- Goschke, T., & Bolte, A. (2014). Emotional modulation of control dilemmas: the role of positive affect, reward, and dopamine in cognitive stability and flexibility. *Neuropsychologia*, 62, 403–423.

- Gramfort, A., Luessi, M., Larson, E., Engemann, D. A., Strohmeier, D., Brodbeck, C., Goj, R., Jas, M., Brooks, T., Parkkonen, L., & Hämäläinen, M. (2013). MEG and EEG data analysis with MNE-Python. *Frontiers in Neuroscience*, 7, 267.
- Gratton, G., Coles, M. G. H., & Donchin, E. (1992). Optimizing the use of information: Strategic control of activation of responses. *Journal of Experimental Psychology. General*, 121(4), 480–506.
- Groen, Y., Priegnitz, U., Fuermaier, A. B. M., Tucha, L., Tucha, O., Aschenbrenner, S., Weisbrod, M., & Garcia Pimenta, M. (2020). Testing the relation between ADHD and hyperfocus experiences. *Research in Developmental Disabilities*, 107(103789), 103789.
- Hauser, T. U., Fiore, V. G., Moutoussis, M., & Dolan, R. J. (2016). Computational Psychiatry of ADHD: Neural Gain Impairments across Marrian Levels of Analysis. *Trends in Neurosciences*, 39(2), 63–73.
- Hayes, T. R., & Petrov, A. A. (2016). Pupil diameter tracks the exploration-exploitation trade-off during analogical reasoning and explains individual differences in fluid intelligence. *Journal of Cognitive Neuroscience*, 28(2), 308–318.
- Holroyd, C. B., & McClure, S. M. (2015). Hierarchical control over effortful behavior by rodent medial frontal cortex: A computational model. *Psychological Review*, 122(1), 54–83.
- Hommel, B. (2015). Between persistence and flexibility. In A. J. Elliot (Ed.), *Advances in Motivation Science* (Vol. 2, pp. 33–67). Elsevier.
- Hong, L., Walz, J. M., & Sajda, P. (2014). Your eyes give you away: prestimulus changes in pupil diameter correlate with poststimulus task-related EEG dynamics. *PloS One*, 9(3), e91321.
- Hubbard, J., Kikumoto, A., & Mayr, U. (2019). EEG Decoding Reveals the Strength and Temporal Dynamics of Goal-Relevant Representations. *Scientific Reports*, 9(1), 1–11.

- Hupfeld, K. E., Abagis, T. R., & Shah, P. (2019). Living “in the zone”: hyperfocus in adult ADHD. *Attention Deficit and Hyperactivity Disorders*, 11(2), 191–208.
- Janitzky, K., Lippert, M. T., Engelhorn, A., Tegtmeier, J., Goldschmidt, J., Heinze, H.-J., & Ohl, F. W. (2015). Optogenetic silencing of locus coeruleus activity in mice impairs cognitive flexibility in an attentional set-shifting task. *Frontiers in Behavioral Neuroscience*, 9, 286.
- Jas, M., Engemann, D. A., Bekhti, Y., Raimondo, F., & Gramfort, A. (2017). Autoreject: Automated artifact rejection for MEG and EEG data. *NeuroImage*, 159, 417–429.
- Jepma, M., & Nieuwenhuis, S. (2011). Pupil diameter predicts changes in the exploration-exploitation trade-off: evidence for the adaptive gain theory. *Journal of Cognitive Neuroscience*, 23(7), 1587–1596.
- Jongkees, B., Todd, M., Lloyd, K., Dayan, P., & Cohen, J. D. (2023). *When it pays to be quick: dissociating control over task preparation and speed-accuracy trade-off in task switching*. <https://psyarxiv.com/quhns/download?format=pdf>
- Joshi, S., & Gold, J. I. (2022). Context-dependent relationships between locus coeruleus firing patterns and coordinated neural activity in the anterior cingulate cortex. *ELife*, 11, e63490.
- Kaiser, J., Oberschulte, J. M., Heckmann, M., & Schütz-Bosbach, S. (2023). Flexible changes in attentional focus and task rules rely on A shared set of frontoparietal oscillatory dynamics. *Journal of Cognitive Neuroscience*, 35(7), 1075–1091.
- Kalanthroff, E., Steinman, S. A., Schmidt, A. B., Campeas, R., & Simpson, H. B. (2018). Piloting a Personalized Computerized Inhibitory Training Program for Individuals with Obsessive-Compulsive Disorder. *Psychotherapy and Psychosomatics*, 87(1), 52–54.

- Kiesel, A., Steinhauser, M., Wendt, M., Falkenstein, M., Jost, K., Philipp, A. M., & Koch, I. (2010). Control and interference in task switching--a review. *Psychological Bulletin*, 136(5), 849–874.
- Klimesch, W., Sauseng, P., & Hanslmayr, S. (2007). EEG alpha oscillations: the inhibition-timing hypothesis. *Brain Research Reviews*, 53(1), 63–88.
- Knapen, T., de Gee, J. W., Brascamp, J., Nuitjen, S., Hoppenbrouwers, S., & Theeuwes, J. (2016). Cognitive and ocular factors jointly determine pupil responses under equiluminance. *PloS One*, 11(5), e0155574.
- Kret, M. E., & Sjak-Shie, E. E. (2019). Preprocessing pupil size data: Guidelines and code. *Behavior Research Methods*, 51(3), 1336–1342.
- Kurzban, R., Duckworth, A., Kable, J. W., & Myers, J. (2013). An opportunity cost model of subjective effort and task performance. *The Behavioral and Brain Sciences*, 36(6), 661–679.
- Lapiz, M. D. S., Bondi, C. O., & Morilak, D. A. (2007). Chronic treatment with desipramine improves cognitive performance of rats in an attentional set-shifting test. *Neuropsychopharmacology: Official Publication of the American College of Neuropsychopharmacology*, 32(5), 1000–1010.
- Liu, C., & Yeung, N. (2020). Dissociating expectancy-based and experience-based control in task switching. *Journal of Experimental Psychology. Human Perception and Performance*, 46(2), 131–154.
- Lloyd, B., de Voogd, L. D., Mäki-Marttunen, V., & Nieuwenhuis, S. (2023). Pupil size reflects activation of subcortical ascending arousal system nuclei during rest. *eLife*, 12. <https://doi.org/10.7554/eLife.84822>

- Macdonald, J. S. P., Mathan, S., & Yeung, N. (2011). Trial-by-trial variations in subjective attentional state are reflected in ongoing prestimulus EEG alpha oscillations. *Frontiers in Psychology*, 2, 82.
- Mather, M., Clewett, D., Sakaki, M., & Harley, C. W. (2016). Norepinephrine ignites local hotspots of neuronal excitation: How arousal amplifies selectivity in perception and memory. *The Behavioral and Brain Sciences*, 39, e200.
- Mathôt, S., & Vilotijević, A. (2022). Methods in cognitive pupillometry: Design, preprocessing, and statistical analysis. *Behavior Research Methods*. <https://doi.org/10.3758/s13428-022-01957-7>
- Mayr, & Grätz. (2024). Does cognitive control have a general stability/flexibility tradeoff problem? *Current Opinion in Behavioral Sciences*, 57(101389), 101389.
- Mayr, & Keele. (2000). Changing internal constraints on action: the role of backward inhibition. *Journal of Experimental Psychology. General*, 129(1), 4–26.
- McBurney-Lin, J., Vargova, G., Garad, M., Zagha, E., & Yang, H. (2022). The locus coeruleus mediates behavioral flexibility. *Cell Reports*, 41(4), 111534.
- McClure, S. M., Gilzenrat, M. S., & Cohen, J. D. (2005). An exploration-exploitation model based on norepinephrine and dopamine activity. *Advances in Neural Information Processing Systems*, 18. [https://papers.nips.cc/paper\\_files/paper/2005/hash/bc4e356fee1972242c8f7eabf4dff517-Abstract.html](https://papers.nips.cc/paper_files/paper/2005/hash/bc4e356fee1972242c8f7eabf4dff517-Abstract.html)
- McMillen, T., & Holmes, P. (2006). The dynamics of choice among multiple alternatives. *Journal of Mathematical Psychology*, 50(1), 30–57.
- Meiran. (1996). Reconfiguration of processing mode prior to task performance. *Journal of Experimental Psychology. Learning, Memory, and Cognition*, 22(6), 1423–1442.

- Meiran. (2000). Modeling cognitive control in task-switching. *Psychological Research*, 63(3–4), 234–249.
- Meyer, D. E., & Kieras, D. E. (1997). A computational theory of executive cognitive processes and multiple-task performance: Part 1. Basic mechanisms. *Psychological Review*, 104(1), 3–65.
- Miletić, S., Turner, B. M., Forstmann, B. U., & van Maanen, L. (2017). Parameter recovery for the Leaky Competing Accumulator model. *Journal of Mathematical Psychology*, 76, 25–50.
- Millan, M. J., Agid, Y., Brüne, M., Bullmore, E. T., Carter, C. S., Clayton, N. S., Connor, R., Davis, S., Deakin, B., DeRubeis, R. J., Dubois, B., Geyer, M. A., Goodwin, G. M., Gorwood, P., Jay, T. M., Joëls, M., Mansuy, I. M., Meyer-Lindenberg, A., Murphy, D., ... Young, L. J. (2012). Cognitive dysfunction in psychiatric disorders: characteristics, causes and the quest for improved therapy. *Nature Reviews. Drug Discovery*, 11(2), 141–168.
- Monsell, S. (2003). Task switching. *Trends in Cognitive Sciences*, 7(3), 134–140.
- Monsell, S., & Mizon, G. A. (2006). Can the task-cuing paradigm measure an endogenous task-set reconfiguration process? *Journal of Experimental Psychology. Human Perception and Performance*, 32(3), 493–516.
- Munn, B. R., Müller, E. J., Wainstein, G., & Shine, J. M. (2021). The ascending arousal system shapes neural dynamics to mediate awareness of cognitive states. *Nature Communications*, 12(1), 6016.
- Murphy, P. R., Boonstra, E., & Nieuwenhuis, S. (2016). Global gain modulation generates time-dependent urgency during perceptual choice in humans. *Nature Communications*, 7, 13526.

- Musslick, S., Bizyaeva, A., Agaron, S., Leonard, N., & Cohen, J. D. (2019). Stability-flexibility dilemma in cognitive control: a dynamical system perspective. *Proceedings of the 41st Annual Meeting of the Cognitive Science Society*. <https://par.nsf.gov/biblio/10125021>
- Musslick, S., & Cohen, J. D. (2021). Rationalizing constraints on the capacity for cognitive control. *Trends in Cognitive Sciences*, 25(9), 757–775.
- Musslick, S., Jang, S. J., Shvartsman, M., & Cohen, J. D. (2018, August 1). Constraints associated with cognitive control and the stability-flexibility dilemma. *Proceedings of the 40th Annual Meeting of the Cognitive Science Society*. <http://dx.doi.org/>
- Nassar, M. R. (2024). Toward a computational role for locus coeruleus/norepinephrine arousal systems. *Current Opinion in Behavioral Sciences*, 59(101407), 101407.
- Nieuwenstein, M. R., Aleman, A., & de Haan, E. H. (2001). Relationship between symptom dimensions and neurocognitive functioning in schizophrenia: a meta-analysis of WCST and CPT studies. Wisconsin Card Sorting Test. Continuous Performance Test. *Journal of Psychiatric Research*, 35(2), 119–125.
- O'Reilly, R. C., & Frank, M. J. (2006). Making working memory work: a computational model of learning in the prefrontal cortex and basal ganglia. *Neural Computation*, 18(2), 283–328.
- Pajkossy, P., Szőllősi, Á., Demeter, G., & Racsmány, M. (2018). Physiological measures of dopaminergic and noradrenergic activity during attentional set shifting and reversal. *Frontiers in Psychology*, 9, 506.
- Pashler, H. (1994). Dual-task interference in simple tasks: Data and theory. *Psychological Bulletin*, 116(2), 220–244.
- Pfeffer, T., Keitel, C., Kluger, D. S., Keitel, A., Russmann, A., Thut, G., Donner, T. H., & Gross, J. (2022). Coupling of pupil- and neuronal population dynamics reveals diverse

influences of arousal on cortical processing. *eLife*, 11.

<https://doi.org/10.7554/eLife.71890>

Pilipenko, A., & Samaha, J. (2024). Double dissociation of spontaneous alpha-band activity and pupil-linked arousal on additive and multiplicative perceptual gain. *The Journal of Neuroscience: The Official Journal of the Society for Neuroscience*, 44(19), e1944232024.

Podvalny, E., King, L. E., & He, B. J. (2021). Spectral signature and behavioral consequence of spontaneous shifts of pupil-linked arousal in human. *eLife*, 10.

<https://doi.org/10.7554/eLife.68265>

Qiao, L., Zhang, L., & Chen, A. (2023). Control dilemma: Evidence of the stability-flexibility trade-off. *International Journal of Psychophysiology: Official Journal of the International Organization of Psychophysiology*, 191, 29–41.

Ratcliff, R. (1978). A theory of memory retrieval. *Psychological Review*, 85(2), 59–108.

Reimer, J., McGinley, M. J., Liu, Y., Rodenkirch, C., Wang, Q., McCormick, D. A., & Tolias, A. S. (2016). Pupil fluctuations track rapid changes in adrenergic and cholinergic activity in cortex. *Nature Communications*, 7, 13289.

Ritz, H., Jha, A., Pillow, J., Daw, N. D., & Cohen, J. D. (2024). Humans actively reconfigure neural task states. In *bioRxiv.org* (p. 2024.09.29.615736).

<https://doi.org/10.1101/2024.09.29.615736>

Ritz, H., & Shenhav, A. (2024). Humans reconfigure target and distractor processing to address distinct task demands. *Psychological Review*, 131(2), 349–372.

Rogers, R. D., & Monsell, S. (1995). Costs of a predictable switch between simple cognitive tasks. *Journal of Experimental Psychology. General*, 124(2), 207–231.

- Sales, A. C., Friston, K. J., Jones, M. W., Pickering, A. E., & Moran, R. J. (2019). Locus Coeruleus tracking of prediction errors optimises cognitive flexibility: An Active Inference model. *PLoS Computational Biology*, 15(1), e1006267.
- Sara, S. J., & Bouret, S. (2012). Orienting and reorienting: the locus coeruleus mediates cognition through arousal. *Neuron*, 76(1), 130–141.
- Seu, E., Lang, A., Rivera, R. J., & Jentsch, J. D. (2009). Inhibition of the norepinephrine transporter improves behavioral flexibility in rats and monkeys. *Psychopharmacology*, 202(1–3), 505–519.
- Shenhav, A., Botvinick, M. M., & Cohen, J. D. (2013). The expected value of control: an integrative theory of anterior cingulate cortex function. *Neuron*, 79(2), 217–240.
- Shenhav, A., Musslick, S., Lieder, F., Kool, W., Griffiths, T. L., Cohen, J. D., & Botvinick, M. M. (2017). Toward a Rational and Mechanistic Account of Mental Effort. *Annual Review of Neuroscience*, 40, 99–124.
- Shiffrin, R. M., & Schneider, W. (1977). Controlled and automatic human information processing: II. Perceptual learning, automatic attending and a general theory. *Psychological Review*, 84(2), 127–190.
- Shine, J. M. (2023). Neuromodulatory control of complex adaptive dynamics in the brain. *Interface Focus*, 13(3), 20220079.
- Shourkeshti, A., Marrocco, G., Jurewicz, K., Moore, T., & Becket Ebitz, R. (2023). Pupil size predicts the onset of exploration in brain and behavior. In *bioRxiv* (p. 2023.05.24.541981). <https://doi.org/10.1101/2023.05.24.541981>
- Siqi-Liu, A., & Egner, T. (2023). Task sets define boundaries of learned cognitive flexibility in list-wide proportion switch manipulations. *Journal of Experimental Psychology. Human Perception and Performance*, 49(8), 1111–1122.

- Siqi-Liu, A., Egner, T., & Woldorff, M. G. (2022). Neural Dynamics of Context-sensitive Adjustments in Cognitive Flexibility. *Journal of Cognitive Neuroscience*, 34(3), 480–494.
- Thura, D., Beauregard-Racine, J., Fradet, C.-W., & Cisek, P. (2012). Decision making by urgency gating: theory and experimental support. *Journal of Neurophysiology*, 108(11), 2912–2930.
- Tromp, J., Nieuwenhuis, S., & Murphy, P. (2022). The Effects of Neural Gain on Reactive Cognitive Control. *Computational Brain & Behavior*, 5(3), 422–433.
- Turner, B. M., & Sederberg, P. B. (2014). A generalized, likelihood-free method for posterior estimation. *Psychonomic Bulletin & Review*, 21(2), 227–250.
- Ueltzhöffer, K., Armbruster-Genç, D. J. N., & Fiebach, C. J. (2015). Stochastic dynamics underlying cognitive stability and flexibility. *PLoS Computational Biology*, 11(6), e1004331.
- Usher, M., & McClelland, J. L. (2001). The time course of perceptual choice: the leaky, competing accumulator model. *Psychological Review*, 108(3), 550–592.
- van Kempen, J., Loughnane, G. M., Newman, D. P., Kelly, S. P., Thiele, A., O'Connell, R. G., & Bellgrove, M. A. (2019). Behavioural and neural signatures of perceptual decision-making are modulated by pupil-linked arousal. *eLife*, 8. <https://doi.org/10.7554/eLife.42541>
- Warren, C. M., Eldar, E., van den Brink, R. L., Tona, K.-D., van der Wee, N. J., Giltay, E. J., van Noorden, M. S., Bosch, J. A., Wilson, R. C., Cohen, J. D., & Nieuwenhuis, S. (2016). Catecholamine-Mediated Increases in Gain Enhance the Precision of Cortical Representations. *The Journal of Neuroscience: The Official Journal of the Society for Neuroscience*, 36(21), 5699–5708.

Waschke, L., Tune, S., & Obleser, J. (2019). Local cortical desynchronization and pupil-linked arousal differentially shape brain states for optimal sensory performance. *eLife*, 8.

<https://doi.org/10.7554/eLife.51501>

Yoo, K., Ahn, J., & Lee, S.-H. (2021). The confounding effects of eye blinking on pupillometry, and their remedy. *PLoS One*, 16(12), e0261463.

Yu, A. J., & Dayan, P. (2005). Uncertainty, neuromodulation, and attention. *Neuron*, 46(4), 681–692.